ARTICLE OPEN

Check for updates

Rasd2 regulates depression-like behaviors via DRD2 neurons in the prelimbic cortex afferent to nucleus accumbens core circuit

Ziqian Cheng[1,2], Fangyi Zhao[1,2], Jingjing Piao[1,2], Wei Yang[1,2], Ranji Cui[1,2]✉ and Bingjin Li[1,2]✉

Depressive symptoms, such as anhedonia, decreased social interaction, and lack of motivation, implicate brain reward systems in the pathophysiology of depression. Exposure to chronic stress impairs the function of brain reward circuits and is well-known to be involved in the etiology of depression. A transcriptomic analysis found that stress alters the expression of *Rasd2* in mice prefrontal cortex (PFC). Similarly, in our previous study, acute fasting decreased *Rasd2* expression in mice PFC, and RASD2 modulated dopamine D2 receptor (DRD2)-mediated antidepressant-like effects in ovariectomized mice. This research suggests the role of RASD2 in stress-induced depression and its underlying neural mechanisms that require further investigation. Here, we show that 5-day unpredictable mild stress (5-d UMS) exposure reduces RASD2 expression in both the nucleus accumbens (NAc) and medial prefrontal cortex (mPFC) of mice, while overexpression (but not knock-down) of *Rasd2* in the NAc core (NAcc) alleviates 5-d UMS-induced depression-like behaviors and activates the DRD2-cAMP-PKA-DARPP-32 signaling pathway. Further studies investigated neuronal projections between the mPFC (Cg1, PrL, and IL) and NAcc, labeled by the retrograde tracer Fluorogold. Depression-like behaviors induced by 5-d UMS were only related to inhibition of the PrL-NAcc circuit. DREADD (Designer receptors exclusively activated by designer drug) analysis found that the activation of PrL-NAcc glutaminergic projection alleviated depression-like behaviors and increased DRD2- and RASD2-positive neurons in the NAcc. Using *Drd2-cre* transgenic mice, we constructed mice with *Rasd2* overexpression in $DRD2^{PrL\text{-}NAcc}$ neurons, finding that *Rasd2* overexpression ameliorated 5-d UMS-induced depression-like behaviors. These findings demonstrate a critical role for RASD2 modulation of $DRD2^{PrL\text{-}NAcc}$ neurons in 5-d UMS-induced depression-like behaviors. In addition, the study identifies a new potential strategy for precision medical treatment of depression.

Molecular Psychiatry (2025) 30:435–449; https://doi.org/10.1038/s41380-024-02684-5

INTRODUCTION

Depression is a major contributor to the overall global burden of disease, with approximately 300 million people worldwide suffering from the disorder, equivalent to 4.4 percent of the world's population [1, 2]. Thus, depression has become a global public health problem that needs to be solved urgently. The symptoms of patients with depression, such as lack of motivation, anhedonia, and decreased social interaction, suggest that brain reward systems are involved in the pathophysiology of depression [3, 4]. Stress, in particular chronic unpredictable stress, affects the processing of reward-related information [5, 6], and attenuates sensitivity to rewarding stimuli in cortical-striatal circuits, that connect the medial prefrontal cortex (mPFC), dorsal striatum, and other brain regions [6–10]. In addition, chronic exposure to unpredictable stressors decreases the levels of dopamine and its metabolites in the nucleus accumbens (NAc) [11], an important modulator of corticostriatal circuits.

Ras homolog enriched in striatum (*Rhes*), also named *Rasd2*, encodes a 266 amino acid protein. Like other Ras superfamily proteins, RASD2 contains five G box domains (termed G1 to G5), recognizing the phosphate moieties of GTP/GDP (G-1 and G-3), the GAP effector (G-2), and the guanine nucleotide moiety (G-4 and G-5) [12–14]. Transcriptomic analysis revealed that chronic mild swim stress alters the expression of *Rasd2* in mouse prefrontal cortex (PFC) [15]. Similarly, in our previous study, 9-hour fasting decreased *Rasd2* expression in mouse PFC, and further studies demonstrated that RASD2 regulates depression-like behaviors via dopamine D2 receptor (DRD2)-related signaling pathways [16]. Recent studies found that RASD2 mainly regulates dopamine receptor signaling pathways in the central nervous system and acts as a modulator of dopamine transmission by regulating the striatal cyclic adenosine monophosphate (cAMP)/protein kinase A (PKA) signaling pathway [13, 17–19]. However, the effect of RASD2 on stress-induced depression and its potential mechanisms have yet to be studied.

Here we used 5-day unpredictable mild stress (5-d UMS) in mice to model the types of chronic stress that humans endure continuously in daily life and are thought to be a predisposing factor for the development of depression [20]. Pharmacological and viral-vector-transgenic approaches demonstrated that there is a critical role for *Rasd2*/RASD2 acting in the NAc in regulating 5-d UMS-induced depression-like behaviors, which are closely linked to the mPFC-NAc neural circuit.

[1]Jilin Provincial Key Laboratory on Molecular and Chemical Genetic, Second Hospital of Jilin University, Changchun 130041, PR China. [2]Engineering Lab on Screening of Antidepressant Drugs, Jilin Province Development and Reform Commission, Changchun 130041, PR China. ✉email: cuiranji@jlu.edu.cn; libingjin@jlu.edu.cn

Received: 12 November 2023 Revised: 18 July 2024 Accepted: 24 July 2024
Published online: 3 August 2024

METHODS

Subjects

Six to eight week-old male C57BL/6J mice were purchased from the Animal Center of Jilin University. *Drd2-cre* mice were kind gifts from Prof. Dongmin Yin (Key Laboratory of Brain Functional Genomics, Ministry of Education and Shanghai, School of Life Science, East China Normal University, Shanghai, China). Specific information on *Drd2-cre* mice is available from the Mutant Mouse Regional Resource Center https://www.mmrrc.org/ (MMRRC # 017263-UCD). *Drd2-cre* mice and wild-type mice used in our studies were 6–8 week-old male mice obtained by crossing *Drd2-cre* transgenic mice with wild-type (C57BL/6J) mice. The mice were housed in 25.5 × 15 × 14 cm cages for 3 days to ensure they were acclimated to the laboratory environment before the study, with a temperature of 23 ± 1 °C, humidity of 40–50%, 12-hour light and dark cycles (7:00–19:00 light cycle), and *ad libitum* food and water. The mice were randomly assigned to each group. All procedures were conducted according to the standards of the Laboratory Animal Guideline for Ethical Review of Animal Welfare (GB/T 35892-2018) and under protocols approved by the Institutional Animal Care and Use Committee of Jilin University.

Experimental design

To investigate the effects of 5-d UMS on depression-like behavior and its related mechanisms, mice were divided into two groups: control group and 5-d UMS group. To investigate the effects of *Rasd2* overexpression (or knock-down) on depression-like behavior and its related mechanisms, mice were divided into ov-control group and ov-*Rasd2* group (or sh-control group and sh-*Rasd2* group), and 5-d UMS were performed 15 days after virus administration. To explore the effects of PrL-NAc core (NAcc) circuit on depression-like behavior and its related mechanism, mice were first divided into control group, hM3Dq group and hM4Di group according to different viral administrations. After 15 days of viral administration, each mouse was exposed to 5-d UMS. Then saline or CNO was administered 30 min before the beginning of behavioral experiments and the above three groups were divided into saline + control, saline + hM3Dq, saline + hM4Di, CNO + control, CNO + hM3Dq and CNO + hM4Di groups. To investigate the effects of *Rasd2* overexpression in $DRD2^{PrL\text{-}NAcc}$ neurons on depression-like behavior, mice were divided into two groups according to genotype: WT group and *Drd2-cre* group. Each group was injected with the same virus.

Surgery

Mice were anesthetized with pentobarbital sodium (65 mg/kg, i.p., Dingguo Changsheng Biotechnology, Beijing, China) and placed in a stereotaxic frame (RWD Life Science, Shenzhen, China). Based on the Paxinos and Franklin mouse brain atlas [21], the NAcc (AP: +1.60; ML: ±1.50; DV: −4.40; mm relative to bregma [22, 23]) and mPFC PrL (AP: +2.10; ML: ±0.35; DV: −2.30; mm relative to bregma [24, 25]) were targeted in separate groups of mice and Fluorogold (or virus) was bilaterally injected into each location at a rate of 0.2 μL/min. After each injection, the needle was left in place for an additional 5 min and then slowly withdrawn. Details of the procedure can be found in a published reference [26].

5-d UMS

Mice received 2–3 of the following stressors each day for 5 consecutive days on a semi-randomized schedule: foot shock for 1 h (0.3 mA, 18 seconds duration at 8-second intervals), restraint for 2 h, exposure to continuous noise (approximately 85 dB [27]) for 8 h, food deprivation for 16 h, water deprivation for 16 h, cage tilt (45 degrees) for 16 h, bedding replaced with damp bedding (1 cm of sawdust and 100 ml of water) for 16 h, bedding (sawdust) removed for 16 h, placed in the cage with 1 cm water for 6 h. The same stressor was not applied on consecutive days.

DREADDs

Mice were anesthetized with pentobarbital sodium (65 mg/kg, i.p., Dingguo Changsheng Biotechnology) and the virus (0.3 μL; CaMKIIa-Cre virus: pAAV2/Retro-CaMKIIa-EGFP-P2A-Cre-WPRE, 3.28E + 12 V.G./mL, Obio Technology) was bilaterally injected into the NAcc and then another virus was bilaterally injected into the PrL region of the mPFC (0.3 μL; control: pAAV2/8-hSyn-DIO-mCherry, 1.34E + 13 V.G./mL; hM4Di: pAAV2/8-hSyn-DIO-hM4D(Gi)-mCherry, 4.43E + 13 V.G./mL; hM3Dq: pAAV2/8-hSyn-DIO-hM3D(Gq)-mCherry, 5.13E + 13 V.G./mL, Obio Technology). 5-d UMS was performed 15 days after the virus injection. Behavioral experiments were performed 30 min after clozapine-N-oxide (CNO) administration (5.0 mg/kg, i.p. [28–30], c0832, Sigma-Aldrich, MI, USA, dissolved in saline at a concentration of 0.5 mg/mL [31]).

Behavioral experiments

Open field test. The circular acrylic apparatus (height: 16 cm) was divided by three concentric circles of diameters 12 cm, 29.4 cm, and 48 cm respectively. Each circle was divided into essentially equal-sized areas. The number of areas in the inner, middle, and outer circles were 1, 5, and 10, respectively. At the beginning of the test, mice were placed individually in the center of a circular acrylic apparatus. The open field test lasted 6 min and was digitally recorded (DCR-SX83E camera, Sony, Shanghai, China). Line crosses (the number of grid lines crossed by the mouse's four paws), rearing (the number of times the mouse stood with its front paws off the ground) and the number of entries in the center square of the apparatus were determined by an observer blinded to the treatment conditions. The total distance moved in the open field test was analyzed by video tracking software (Noldus, Wageningen, the Netherlands, EthoVision XT 13). Details of the procedure can be found in published references [16, 32].

Forced swimming test. Mice were individually placed in a cylindrical container (height: 25 cm; diameter: 11 cm) containing 12 cm of water (temperature: 25 ± 1 °C). The test lasted 6 min and was digitally recorded by a camera (Sony, DCR-SX83E). The first two minutes were considered as acclimatization time. Behavior was only assessed during the last 4 min of the test. The time spent immobile (defined by lack of any movement except that necessary to keep the head out of the water), swimming (defined by swimming movements parallel to the sides of the container), and climbing (defined by climbing movements with the mouse oriented perpendicularly toward the sides of the container) [33], as well as defecation (number of fecal boli), were analyzed by an observer blinded to the treatment conditions. Details of the procedure can be found in published references [16, 32].

Sucrose preference test. Mice were adapted to consuming 1% sucrose solution for 2 days before the formal test (mice were given two bottles of 1% sucrose solution per test cage). Mice were deprived of water for 12 h, then two weighed bottles (one for 1% sucrose solution and one for water) were placed in each cage. The bottles were weighed at several time points, 07:00, 08:00, 09:00, 10:00, 13:00, and 19:00. The starting positions of the two bottles were initially randomized, exchanged after each weighing, and the sucrose solution and water consumption were measured at the noted time-points. Sucrose preference was calculated as sucrose solution consumption / (sucrose solution consumption + water consumption) × 100%. Details of the procedure can be found in published references [16, 34].

Tail suspension test. Tape was placed 2 cm from the tip of the mouse's tail and the mouse was affixed to a horizontal metal bar in an inverted state with the head approximately 20 cm above a benchtop. The behavior of mice over 5 min was recorded by a camera (Sony, DCR-SX83E). Immobility time (the time the mouse stopped all struggling movements, in a vertical position, and immobile) was analyzed in the last 4 min of the test by an observer blinded to treatment conditions. Details of the procedure can be found in published references [16, 34, 35].

Enzyme-linked immunosorbent assay

Blood was collected by retro-orbital bleeding and placed at room temperature for 1 h, followed by centrifugation at 3000 rpm for 10 min. Then the serum was collected and stored at −80 °C until analysis. The serum concentration of corticosterone was quantified according to the recommended protocol (FY2061-A corticosterone kit, Feiya Biotechnology, Jiangsu, China). The optical density of the samples was recorded at 450 nm using a microtiter plate reader (Thermo Scientific, MA, USA, Varioskan Flash) for 15 min, and the concentration was determined from the regression line for a standard curve run at the same time.

Western blotting

Mice were decapitated after being anesthetized with pentobarbital sodium (65 mg/kg, i.p., Dingguo Changsheng Biotechnology). The whole brain was removed and placed on dry ice in a stainless-steel brain matrix (RWD Life Science, 68707), and the brain was cut into 1 mm thick coronal slices using a razor blade [36]. Bilateral NAc and mPFC were dissected according to the mouse brain atlas [21] and stored at −80 °C until further analysis. The

tissue was homogenized in RIPA buffer (R0020, Solarbio, Beijing, China) with 1% phenylmethylsulphonyl fluoride solution, and the supernatant was obtained after centrifugation at 12,000 rpm for 20 min at 4 °C. After mixing with the loading buffer, the sample vials were placed in boiling water for 5 min. The sample was loaded onto 5% sodium dodecyl sulfate-polyacrylamide electrophoresis (SDS-PAGE) gels and proteins separated by electrophoresis at 110 constant voltage (Bio-Rad, CA, USA PowerPac, Universal). To analyze target proteins, the gels were transferred to polyvinylidene difluoride membranes (IPVH00010, Millipore, MA, USA) at 110 constant voltage for 1 h and then followed by blocking with 5% skim-milk (dissolved in Tris-buffered saline (TBS)) for 2 h. The membranes were incubated in TBS containing primary antibody at 4 °C overnight: RASD2 (1:800, rabbit polyclonal antibody, ab67277, Abcam, Cambridge, UK); DRD1 (1:800, rabbit polyclonal antibody, DF7097, Affinity, OH, USA); DRD2 (1:1000, rabbit polyclonal antibody, ab130295, Abcam); DARPP-32 (PPP1R1B; 1:1000, rabbit monoclonal antibody, #2306, Cell Signaling Technology, MA, USA); GluA1 (GRIA1; 1:2000, rabbit polyclonal antibody, ab109450, Abcam); β-actin (ACTB; 1:2000, mouse monoclonal antibody, HC201, TransGen Biotech, Beijing, China); cAMP (1:2000, rabbit polyclonal antibody, ab26322, Abcam); PKA (PRKACA; 1:3000, rabbit polyclonal antibody, ab75991, Abcam); and GAPDH (1:3000, mouse monoclonal antibody, HC301, TransGen Biotech). After washing in TBST (TBS containing 0.1% Tween-20), the membranes were incubated in TBS containing secondary antibody for 1 h at room temperature (anti-rabbit: 1:2000, ZB2301, ZSBG-Bio, Beijing, China; or anti-mouse: 1:5000, ZB2305, ZSBG-Bio; as appropriate). After washing with TBST, bands were detected with enhanced chemiluminescence supersensitive developer solution (WBKLS0500, Millipore) and analyzed by Image J software, version 1.52.

Co-immunoprecipitation

In the co-immunoprecipitation procedure, the steps for brain tissue acquisition and protein extraction were the same as for western blotting. Co-immunoprecipitation was quantified using the recommended protocol (abs995, Absin, Shanghai, China). Firstly, 5 µL of Protein A and 5 µL of Protein G were added to 500 µL of sample and incubated for 60 min at 4 °C, followed by centrifugation at 12,000 × *g* for 1 minute at 4 °C, and removal of the supernatant. 1 µg of primary antibody (RASD2, rabbit polyclonal antibody, RHES-101AP, FabGennix, TX, USA; or Rabbit IgG, abs20035, Absin; as appropriate) was added to the supernatant and incubated overnight at 4 °C with gentle mixing. After washing with 500 µL wash buffer (1×), the samples were centrifuged at 12,000 × *g* for 1 min and the precipitate was retained. Forty µL of SDS sample buffer (1×) was added to the precipitate and then the samples were placed in a water bath for 5 min at 95–100 °C, followed by centrifugation at 14,000 × *g* for 1 minute. Finally, the samples were analyzed by western blotting (primary antibody: RASD2, 1:500, RHES-101AP, rabbit polyclonal antibody, FabGennix; DRD2, 1:500, sc-5303, mouse monoclonal antibody, Santa Cruz Bio, TX, USA).

Immunohistochemistry

On the 3rd day after the last 5-d UMS, 90 min after the last behavioral experiment, the whole brains of mice were removed for immunostaining. Mice were anesthetized by intraperitoneal injection with pentobarbital sodium (65 mg/kg, Dingguo Changsheng Biotechnology), and then perfused transcardially with saline followed by 4% paraformaldehyde at 4 °C. After perfusion, mouse brains were removed, post-fixed in 4% paraformaldehyde for 24 h at 4 °C, and then transferred to 30% sucrose solution in 0.1 M PBS until sinking. Next, the brain tissue was placed in a tinfoil box containing Tissue-Tek O.C.T. Compound (#4583, SAKURA, CA, USA), and stored at −80 °C for further analysis. Coronal sections (30 µm thickness) of brain tissue were taken using a cryostat (Leica, Heidelberg, Germany, CM1860). The brain slices were washed in PBS, transferred to PBS containing 0.6% hydrogen peroxide and incubated at room temperature for 15 min. After washing with PBS, the brain slices were transferred to a solution containing the primary antibody (c-Fos, 1:1000, mouse monoclonal antibody, sc-166940, Santa Cruz Bio; RASD2, 1:500, rabbit polyclonal antibody, ab67277, Abcam), 2% normal goat serum (abs933, Absin), 0.05% sodium azide and 0.3% Triton X-100 PBS, and incubated at 4 °C for 72 h. After washing with PBS, the slices were transferred to a solution containing secondary antibody (goat anti-rabbit (HRP conjugated), 1:400, ZB2010, ZSBG-Bio; or goat anti-mouse (HRP conjugated), 1:400, CW0102S, CWBIO, Beijing, China; as appropriate) and 0.3% Triton X-100 PBS, incubated at room temperature for 75 min, and then washed in PBS. The brain slices were incubated using the VECTASTAIN ABC kit (PK4002, Vector Laboratories, CA, USA) for 75 min and then washed with PBS, followed by processing with the DAB Substrate Kit (BL732A, Biosharp Life Sciences, Anhui, China), and incubated for 10 min. After washing with PBS, slices were placed on microscope slides and stained in 0.2% neutral red solution for 3 min. The reaction was terminated with ddH_2O, and the slides were soaked for 15 s each in 70%, 95%, and 100% ethanol solutions, followed by xylene for 1 min. Slides were sealed with neutral gum. The staining was observed and captured by microscope (Olympus, Japan, IX73/BX51WI). Counting of c-Fos nuclei was conducted by individuals blinded to experimental conditions. Each count is the average of triplicate measures. Details of the procedure can be found in a published reference [26].

Immunofluorescence

The methods of obtaining and fixing brain tissue followed procedures described for immunohistochemistry. Brain tissues were coronally sectioned on a cryostat (Leica, CM1860) at a thickness of 15 µm, attached to slides, dried at room temperature, and stored at −20 °C for later processing. After washing with PBS, the slices were placed in citrate buffer (1×) (CW0128S, CWBIO) and microwaved to retrieve antigens. Slices were transferred to a solution containing 10% normal goat serum in 0.3% Triton X-100 PBS and incubated at room temperature for 2 h. Brain slices were transferred to solutions containing a primary antibody in 0.15% Triton X-100 PBS and 1.5% normal goat serum, and incubated at 4 °C overnight. The primary antibodies used were: c-Fos (1:50, mouse monoclonal antibody, sc-166940, Santa Cruz Bio; 1:500, Rabbit monoclonal, ab214672, Abcam), Fluorescent Gold (1:1000, rabbit polyclonal antibody, AB153-I, Millipore Sigma, PA, USA), RASD2 (1:200, rabbit polyclonal antibody, ab67277, Abcam), DRD2 (1:50, mouse monoclonal antibody, sc-5303, Santa Cruz Bio). After incubation in primary antibodies, slices were washed with PBS and incubated with the secondary antibody in 0.15% Triton X-100 PBS for 1 h at room temperature. The secondary antibodies used were: FITC Goat Anti-Rabbit (1:1000, RS0004, ImmunoWay Biotechnology), Alexa Fluor® 594 Goat Anti-Mouse (1:200, ab150116, Abcam), Alexa Fluor® 488 Goat Anti-Mouse (1:2000, ab150113, Abcam), Cy3 Goat Anti-Rabbit (1:100, AS007, ABclonal Technology, Wuhan, China). Following DAPI staining for 5 min, the slices were washed with PBS and sealed with 30% glycerol. The staining was observed and captured by microscope (IX73/BX51WI, Olympus). The positive cells with fluorescence were counted by Image J software, version 1.52. Each count is the average of triplicate measures.

Statistical analysis

No statistical methods were used to predetermine sample sizes in mouse studies, but our sample sizes are similar to those reported in previous publications [30, 37, 38]. Data were represented as mean ± s.e.m. and were analyzed using GraphPad Prism software (version 8.0.1) and SPSS (version 23). For all two group experiments, two-tailed unpaired *t*-tests were used. For more than 2 group experiments, two-way and three-way ANOVA were used to compare the effects of factorial designs. When a significant difference was obtained in ANOVA, *post hoc* comparisons were performed between means using Tukey's HSD test. $p < 0.05$ was considered statistically significant. The Shapiro–Wilk test was used to evaluate the normality of the data. All statistical tests were two-sided.

RESULTS

5-d UMS was sufficient to induce depression-like behaviors in mice

To investigate whether 5-d UMS produced depression-like behavior, behavioral changes were analyzed (Fig. 1a). In the open field test, there were no significant differences between control and 5-d UMS mice in the total distance moved, line crosses, rearing, or center entries (Fig. 1b–g), suggesting that 5-d UMS exposure had no effect on locomotor activity. The forced swim test, sucrose preference test, and tail suspension test were performed to evaluate depression-like behavior. Antidepressants selectively increase climbing behavior in the forced swim test in animals through the catecholaminergic systems, while antidepressants targeting the serotonergic system selectively increase swimming behavior [39, 40], therefore, we conducted a detailed analysis of behavior in the forced swim test. The results showed that the duration of immobility was increased after 5-d UMS, while the duration of climbing and swimming was decreased (Fig. 1h–j).

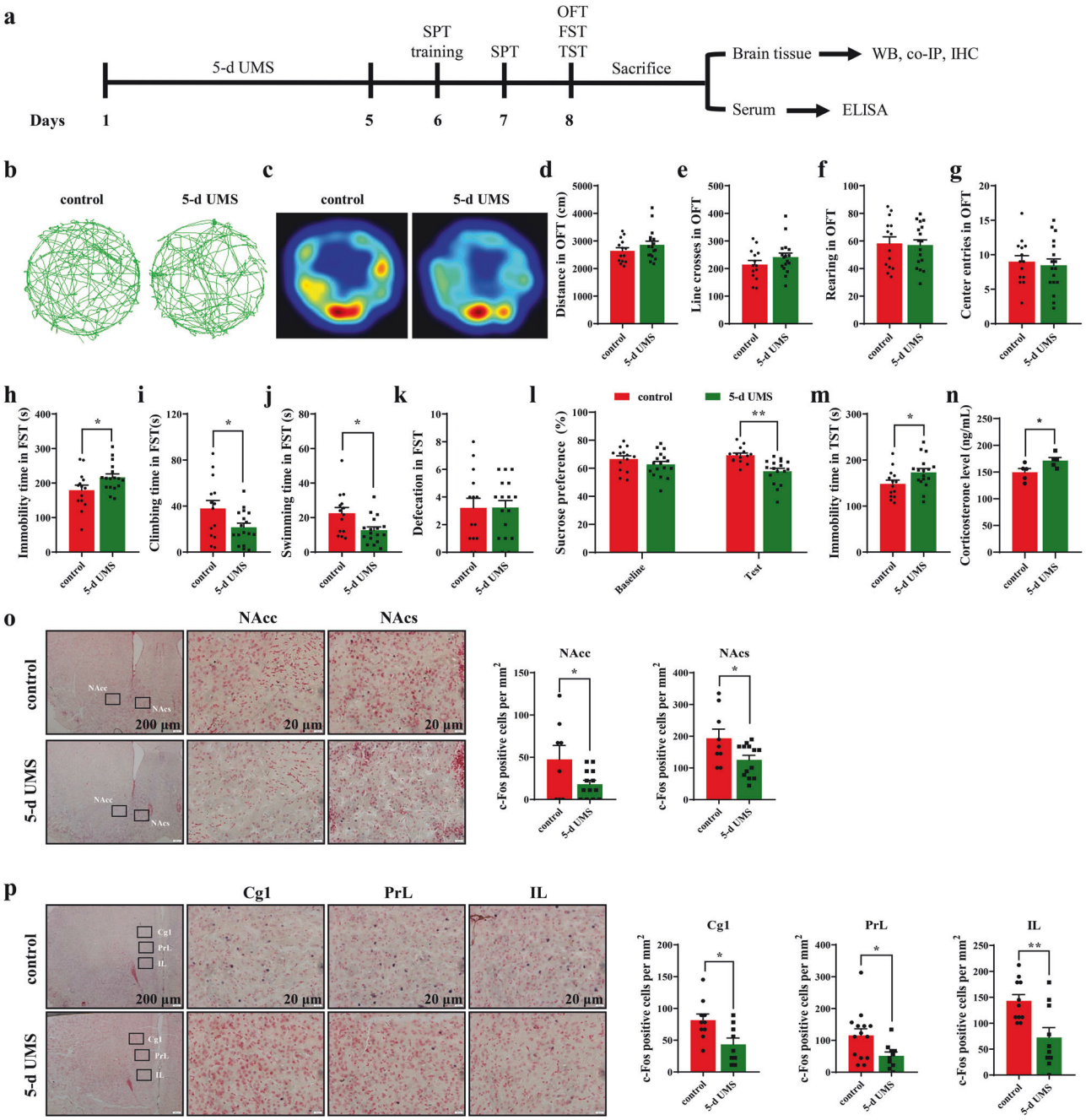

Fig. 1 5-d UMS exposure induces depression-like behavior in mice. a Schematic of experimental design and timeline. Representative tracks (**b**) and heatmaps (**c**) displaying mouse movement in the open field test. Total distance of movement (**d**), line crosses (**e**), rearing (**f**), and center entries (**g**) in the open field test. $N = 14$ and 17 mice for control and 5-d UMS groups, respectively. Two-tailed unpaired *t*-test: distance, $t_{(29)} = 1.214$, $p = 0.2347$; line crosses, $t_{(29)} = 1.286$, $p = 0.2088$; rearing, $t_{(29)} = 0.1964$, $p = 0.8457$; and center entries, $t_{(29)} = 0.4110$, $p = 0.6841$. The immobility time (**h**), climbing time (**i**), swimming time (**j**), and defecation (fecal boli) (**k**) in the forced swim test. $N = 14$ and 17 mice for control and 5-d UMS groups, respectively. Two-tailed unpaired *t*-test: immobility time, $t_{(29)} = 2.172$, $p = 0.0382$; climbing time, $t_{(29)} = 2.220$, $p = 0.0344$; swimming time, $t_{(29)} = 2.682$, $p = 0.0119$; defecation, $t_{(29)} = 0.02498$, $p = 0.9802$. **l** Graph represents sucrose preference data (%) during baseline (Day 0) and treatment (Day 7) phases of the study. $N = 14$ and 17 mice for control and 5-d UMS groups, respectively. Two-way ANOVA (factor 1: time; factor 2: treatment): $F_{\text{time×treatment }(1,\ 58)} = 3.348$, $p = 0.0724$; $F_{\text{time }(1,\ 58)} = 0.2884$, $p = 0.5933$; $F_{\text{treatment }(1,\ 58)} = 13.40$, $p = 0.0005$. Tukey's HSD post hoc test: after treatment, $p_{(\text{control vs. 5-d UMS})} = 0.0015$. **m** Immobility time in the tail suspension test. $N = 14$ and 17 mice for control and 5-d UMS groups, respectively. Two-tailed unpaired *t*-test: $t_{(29)} = 2.136$, $p = 0.0413$. **n** Corticosterone levels in mouse serum ($n = 5$ per group). $t_{(8)} = 2.415$, $p = 0.0422$. **o** Representative images showing c-Fos expression in the NAc (left, scale bar, 200 and 20 μm) and the number of c-Fos expressing neurons in NAcc and NAcs (right). $N = 3$ and 4 mice for control and 5-d UMS groups respectively. Two-tailed unpaired *t*-test: NAcc, $t_{(19)} = 2.097$, $p = 0.0496$; NAcs, $t_{(20)} = 2.326$, $p = 0.0307$. **p** Representative images showing c-Fos expression in the mPFC (left, scale bar 200 and 20 μm), and the number of c-Fos expressing neurons in Cg1, PrL, and IL (right). $N = 4$ and 3 mice for control and 5-d UMS groups, respectively. Two-tailed unpaired *t*-test: Cg1, $t_{(17)} = 2.738$, $p = 0.0140$; PrL, $t_{(22)} = 2.405$, $p = 0.0250$; IL, $t_{(19)} = 3.199$, $p = 0.0047$. The data are expressed as mean ± s.e.m. $^{*}p < 0.05$, $^{**}p < 0.01$ and $^{***}p < 0.001$. 5-d UMS 5-day unpredictable mild stress, OFT open field test, FST forced swim test, TST tail suspension test, WB western blotting, co-IP co-immunoprecipitation, IHC immunohistochemistry, ELISA enzyme-linked immunosorbent assay, NAcc NAc core, NAcs NAc shell, Cg1 cingulate cortex 1, PrL prelimbic cortex, IL infralimbic cortex.

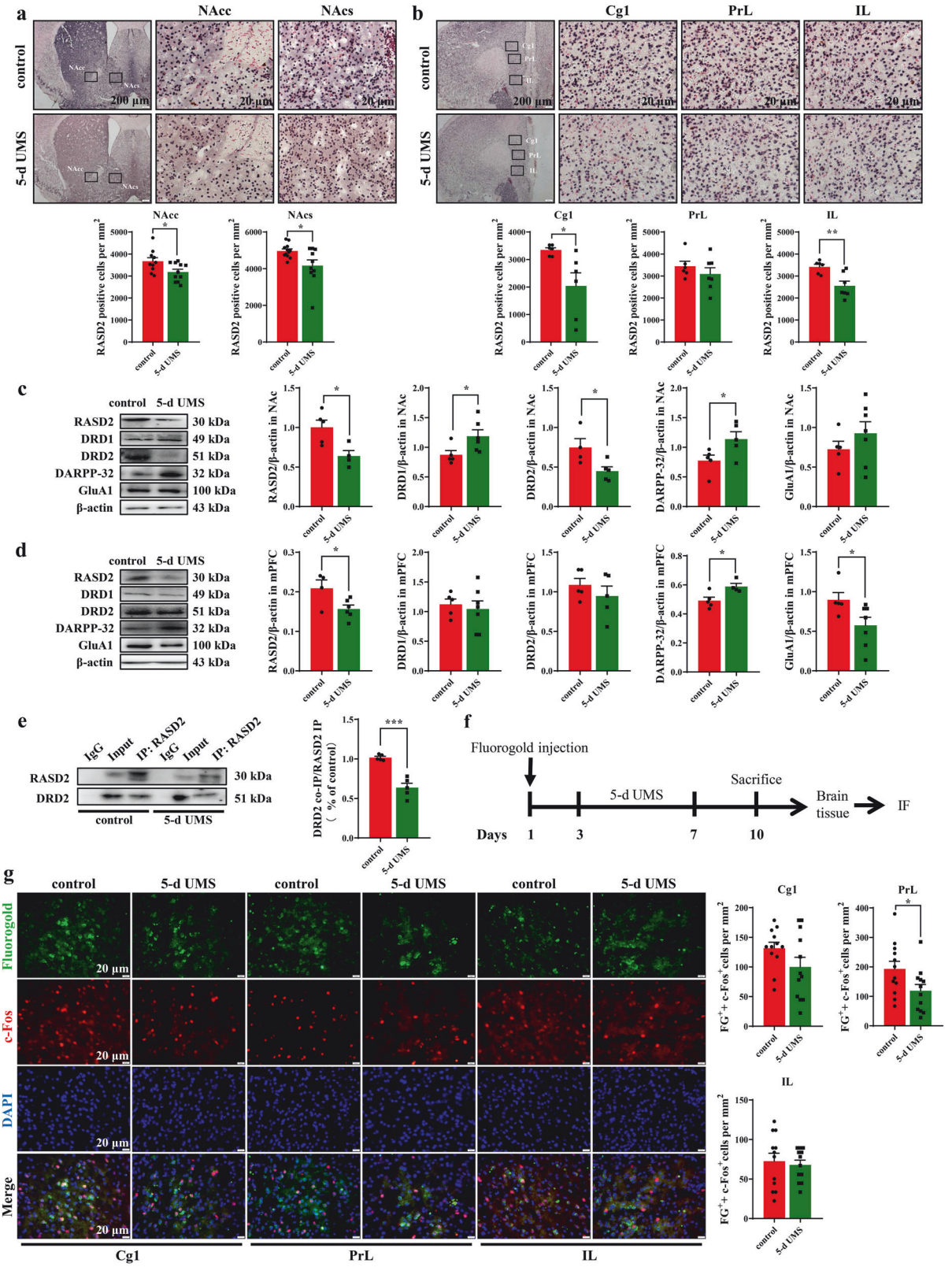

In addition, 5-d UMS exposure significantly reduced sucrose preference in mice (Fig. 1l) and increased immobility time in the tail suspension test (Fig. 1m). These results suggest that 5-d UMS exposure induces depression-like behavior in mice.

To further confirm the 5-d UMS-induced mouse depression model, we measured plasma corticosterone levels by an enzyme-linked immunosorbent assay, finding that 5-d UMS exposure significantly increased serum corticosterone levels (Fig. 1n). This is

Fig. 2 The mechanisms of 5-d UMS in inducing depression-like behavior involve RASD2 and DRD2. a The representative images showing RASD2 expression in the NAc (top, scale bar = 200 and 20 μm), and the number of RASD2-expressing neurons in NAcc and NAcs (bottom). $N = 4$ mice per group. Two-tailed unpaired *t*-test: NAcc, $t_{(19)} = 2.418$, $p = 0.0258$; NAcs, $t_{(20)} = 2.591$, $p = 0.0175$. **b** Representative images showing RASD2 expression in the mPFC (top, scale bar = 200 and 20 μm), and the number of RASD2-expressing neurons in Cg1, PrL, and IL (bottom). $N = 3$ mice per group. Two-tailed unpaired *t*-test: Cg1, $t_{(10)} = 2.721$, $p = 0.0215$; PrL, $t_{(11)} = 0.9488$, $p = 0.3631$; IL, $t_{(11)} = 3.407$, $p = 0.0059$. **c** 5-d UMS caused changes in RASD2 and dopamine-related protein expression in the NAc. $N = 4$–7 mice. Two-tailed unpaired *t*-test: RASD2, $t_{(7)} = 3.050$, $p = 0.0186$; DRD1, $t_{(9)} = 2.315$, $p = 0.0458$; DRD2, $t_{(7)} = 2.597$, $p = 0.0356$; DARPP-32, $t_{(8)} = 2.313$, $p = 0.0494$; GluA1, $t_{(10)} = 1.035$, $p = 0.3251$. **d** 5-d UMS caused changes in RASD2 and dopamine-related protein expression in the mPFC. $N = 4$–7 mice. Two-tailed unpaired *t*-test: RASD2, $t_{(8)} = 2.507$, $p = 0.0365$; DRD1, $t_{(10)} = 0.4337$, $p = 0.6737$; DRD2, $t_{(8)} = 0.9415$, $p = 0.3740$; DARPP-32, $t_{(7)} = 2.981$, $p = 0.0205$; GluA1, $t_{(10)} = 2.250$, $p = 0.0482$. **e** Western blot images of a RASD2 immunoprecipitation showing co-immunoprecipitation of RASD2 and DRD2 in the NAc (left). Quantification of DRD2 co-immunoprecipitation with RASD2 immunoprecipitation. Each sample was normalized by its input and then DRD2 was normalized for the amount of RASD2 immunoprecipitated (right). $N = 5$ mice per group. Two-tailed unpaired *t*-test: $t_{(8)} = 6.616$, $p = 0.0002$. **f** Schematic of experimental design and timeline. **g** 5-d UMS reduces the projection of PrL to the NAcc (scale bar, 20 μm). $N = 4$ mice per group. Two-tailed unpaired *t*-test: Cg1, $t_{(22)} = 1.665$, $p = 0.1102$; PrL, $t_{(22)} = 2.202$, $p = 0.0385$; IL, $t_{(22)} = 0.4018$, $p = 0.6917$. The data are expressed as mean ± s.e.m. $^{*}p < 0.05$, $^{**}p < 0.01$ and $^{***}p < 0.01$. 5-d UMS 5-day unpredictable mild stress, IF immunofluorescence, DRD1 dopamine D1 receptor, DRD2 dopamine D2 receptor, DARPP-32 dopamine and cAMP-regulated phosphoprotein, 32 kDa, GluA1 glutamate receptor subunit 1, FG fluorogold, NAcc NAc core, NAcs NAc shell, Cg1 cingulate cortex 1, PrL prelimbic cortex, IL infralimbic cortex.

consistent with previous studies that stress induces elevated plasma corticosterone levels in mice [41, 42]. In addition, immunohistochemistry was performed to investigate the changes in c-Fos expression in the NAc and mPFC, and the results showed that 5-d UMS exposure significantly reduced c-Fos expression in the NAc (core and shell) and mPFC (Cg1, PrL, and IL) (Fig. 1o, p). The above results indicate that the 5-d UMS depression model recapitulated several features of depression.

5-d UMS reduces RASD2 protein expression in the NAc and mPFC and regulates the levels of RASD2-related proteins

To further investigate the molecular mechanisms related to 5-d UMS-induced depression-like behavior, we first explored the changes in RASD2 protein expression in the NAc and mPFC by immunohistochemistry. We found that 5-d UMS significantly reduced the expression of RASD2 in the NAc (core and shell) (Fig. 2a) and reduced the expression of RASD2 in the Cg1 and IL subregions of the mPFC (Fig. 2b).

Based on the critical regulatory role of dopamine receptor-related signaling pathways in depression-like behaviors, and the role of RASD2 in the regulation of dopamine receptor function [17, 43–45], western blotting was performed to investigate the effects of 5-d UMS on the protein levels of RASD2, DRD1, DRD2, DARPP-32, and GluA1 in the NAc and mPFC. There was a decrease in RASD2 and DRD2 expression, while there was an increase in DRD1 and DARPP-32 expression in the NAc of mice after 5-d UMS (Fig. 2c). In addition, there was a decrease in RASD2 and GluA1 expression, while there was an increase in DARPP-32 expression in the mPFC of mice after 5-d UMS (Fig. 2d). To explored the effect of 5-d UMS on the interaction between RASD2 and DRD2 in the NAc, co-immunoprecipitation was performed, providing evidence for a direct interaction between RASD2 and DRD2 in the NAc, which was reduced by 5-d UMS (Fig. 2e).

5-d UMS inhibits the projection of PrL to the NAcc

There are differential projections to NAc subregions from cortical and subcortical structures. For instance, PFC preferentially projects to NAcc and ventral hippocampus preferentially projects to NAc shell (NAcs) [25, 46]. To label mPFC neuronal pathways projecting to the NAcc, and to explore the effect of 5-d UMS on this circuit, we injected the Fluorogold bilaterally into the NAcc. Two days after the injection, the mice experienced 5-d UMS or went unstressed (Fig. 2f). Fluorogold-positive neurons in the NAcc reversely labeled neurons in the mPFC which were co-labeled with c-Fos by immunofluorescence. As shown in Fig. 2g, there was Fluorogold labeling in all three mPFC subregions (Cg1, PrL, and IL). 5-d UMS significantly reduced the co-expression of c-Fos and Fluorogold in the PrL. Collectively, these results indicate that all three subregions in the mPFC send projections to the NAcc, but 5-d UMS only inhibits activity in the PrL-NAcc circuit.

Rasd2 overexpression in NAcc alleviates depression-like behaviors after 5-d UMS

Since RASD2 is mainly concentrated in the striatum [17] and 5-d UMS induced changes in DRD1 and DRD2 expression in the NAc (but not mPFC), we constructed mice with *Rasd2* overexpression or knock-down in the NAcc by injecting lentivirus vectors bilaterally into the NAc (1.0 μL; ov-control: pLenti-Ubc-EGFP-3FLAG, 1.55E + 09 TU/mL; ov-*Rasd2*: pLenti-Ubc-EGFP-2A-3FLAG-Rasd2, 4.77E + 08 TU/mL, Obio Technology, Shanghai, China) (1.0 μL; sh-control: pLV-hU6-NC-hef1a-mNeongreen-P2A-Puro, 2.82E + 08 TU/mL; sh-*Rasd2*: pLV-hU6-Rasd2-hef1a-mNeongreen-P2A-Puro, 2.68E + 08 TU/mL, Synthetic Biological Technology, Beijing, China) (Fig. 3b and Supplementary Fig. 1b). The 5-d UMS exposure started 15 days after virus injection. Subsequently, behavioral experiments were performed to explore the effects of *Rasd2* manipulations on depression-like behavior after 5-d UMS (Fig. 3a and Supplementary Fig. 1a). In the open field test, *Rasd2* overexpression (or knock-down) in NAcc had no significant effect on the total distance moved, line crosses, rearing, or center entries (Fig. 3g–l and Supplementary Fig. 1g–l), indicating that *Rasd2* overexpression (or knock-down) in the NAcc had no effect on locomotor activity after 5-d UMS. In the forced swim test, *Rasd2* overexpression significantly reduced the duration of immobility (Fig. 3c), the duration of climbing (Fig. 3d), and defecation (Fig. 3f), but significantly increased the duration of swimming after 5-d UMS (Fig. 3e). *Rasd2* overexpression in the NAcc also significantly increased sucrose preference (Fig. 3m) and decreased immobility in the tail suspension test after 5-d UMS (Fig. 3n). However, *Rasd2* knock-down in the NAcc had no effect on depression-like behaviors after 5-d UMS (Supplementary Fig. 1c–f, m–n).

Rasd2 overexpression in the NAcc activates DRD2-cAMP-PKA-DARPP-32 signaling pathways after 5-d UMS

To expand upon the above experimental results showing that 5-d UMS reduced GluA1 protein expression in the mPFC, we next investigated the effects of *Rasd2* overexpression (or knock-down) on the expression of GluA1 in the mPFC after 5-d UMS. The results showed that *Rasd2* overexpression increased GluA1 protein expression in the mPFC (Fig. 3o).

Based on the key regulatory role of the DRD1/DRD2-cAMP-PKA-DARPP-32 signaling pathway in antidepressant-like effects, we next investigated molecular changes in the expression of related proteins in the NAc and mPFC after *Rasd2* overexpression (or knock-down). The results showed that *Rasd2* overexpression increased the expression of DRD2 and significantly decreased

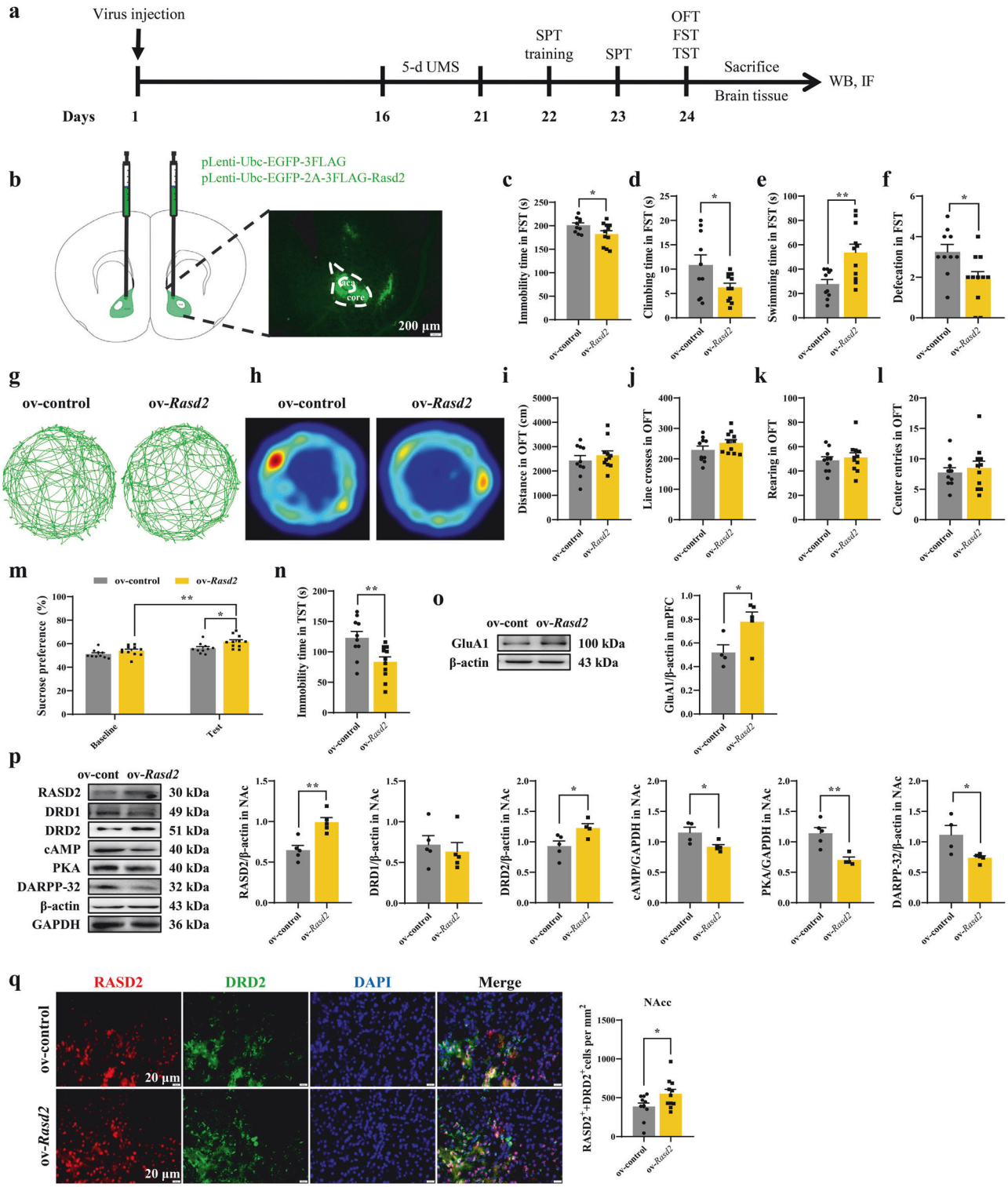

the expression of cAMP, PKA, and DARPP-32 in the NAc (Fig. 3p). However, knock-down of *Rasd2* only reduced DRD2 expression in the NAc (Supplementary Fig. 1p).

To further confirm that the role of *Rasd2* overexpression in the NAcc in regulating depression-like behavior after 5-d UMS is related to DRD2 signaling, we investigated the effect of *Rasd2* overexpression on the colocalization of RASD2 and DRD2 by immunofluorescence. The results showed that *Rasd2* overexpression increased co-labeling of DRD2 and RASD2 in the NAcc (Fig. 3q).

Activation of PrL-NAcc glutaminergic projection alleviates depression-like behaviors and increases DRD2- and RASD2-positive neurons in the NAcc

Our results show that 5-d UMS decreased the expression of GluA1 in the mPFC and inhibited the PrL-NAcc circuit. Previous work has

Fig. 3 ***Rasd2*** **overexpression in the NAcc attenuates depression-like behavior and activates the DRD2-cAMP-PKA-DARPP-32 signaling pathway in mice. a** Schematic of experimental design and timeline. **b** Schematic diagram of microinjection of lentivirus vectors into mouse NAcc. Duration of immobility (**c**), climbing (**d**), and swimming (**e**), and the number of fecal boli (defecation) (**f**) in the forced swim test. $N = 10$, 11 mice in ov-control and ov-*Rasd2* groups, respectively. Two-tailed unpaired *t*-test: duration of immobility, $t_{(19)} = 2.100$, $p = 0.0493$; duration of climbing, $t_{(19)} = 2.130$, $p = 0.0465$; duration of swimming, $t_{(19)} = 3.216$, $p = 0.0046$; defecation, $t_{(19)} = 2.590$, $p = 0.0180$. Representative tracks (**g**) and heatmaps (**h**) displaying mouse movement in the open field test. Total distance moves (**i**), line crosses (**j**), rearing (**k**), and center entries (**l**) in the open field test. $N = 10$, 11 mice for ov-control and ov-*Rasd2* groups, respectively. Two-tailed unpaired *t*-test: distance, $t_{(19)} = 0.8095$, $p = 0.4282$; line crosses, $t_{(19)} = 1.413$, $p = 0.1737$; rearing, $t_{(19)} = 0.5033$, $p = 0.6206$; center entries, $t_{(19)} = 0.5485$, $p = 0.5897$. **m** Graph represents sucrose preference (%) before (Day 0) and after (Day 23) 5-d UMS. $N = 10$, 11 mice for ov-control and ov-*Rasd2* groups, respectively. Two-way ANOVA (factor 1: time; factor 2: treatment): $F_{\text{timextreatment (1, 38)}} = 0.9972$, $p = 0.3243$; $F_{\text{time (1, 38)}} = 21.83$, $p < 0.0001$; $F_{\text{treatment (1,38)}} = 9.783$, $p = 0.0034$. Tukey's HSD post hoc test: after treatment, $p_{\text{(ov-control vs. ov-}Rasd2\text{)}} = 0.0288$; in the ov-*Rasd2* mice, $p_{\text{(baseline vs. test)}} = 0.0011$. **n** Duration of immobility in the tail suspension test. $N = 10$, 11 mice in ov-control and ov-*Rasd2* groups, respectively. Two-tailed unpaired *t*-test: $t_{(19)} = 3.015$, $p = 0.0071$. **o** *Rasd2* overexpression in the NAcc increased the GluA1 expression in the mPFC after 5-d UMS. $N = 4$, 5 mice in ov-control and ov-*Rasd2* groups, respectively. Two-tailed unpaired *t*-test: $t_{(7)} = 2.391$, $p = 0.0481$. **p** *Rasd2* overexpression activated the DRD2-cAMP-PKA-DARPP-32 signaling pathway in the NAc. $N = 4$-5 mice. Two-tailed unpaired *t*-test: RASD2, $t_{(8)} = 4.255$, $p = 0.0028$; DRD1, $t_{(8)} = 0.5450$, $p = 0.6006$; DRD2, $t_{(7)} = 2.591$, $p = 0.0359$; cAMP, $t_{(7)} = 2.692$, $p = 0.0310$; PKA, $t_{(7)} = 3.887$, $p = 0.0060$; DARPP-32, $t_{(7)} = 2.689$, $p = 0.0311$. **q** *Rasd2* overexpression increased the co-expression of RASD2 and DRD2 (scale bar, 20 μm). $N = 4$ mice per group. Two-tailed unpaired *t*-test: $t_{(20)} = 2.270$, $p = 0.0344$. The data are expressed as mean ± s.e.m. $^*p < 0.05$ and $^{**}p < 0.01$. 5-d UMS 5-day unpredictable mild stress, OFT open field test, FST forced swimming test, TST tail suspension test, WB western blotting, IF immunofluorescence, GluA1 glutamate receptor subunit 1, DRD1 dopamine D1 receptor, DRD2 dopamine D2 receptor, cAMP cyclic adenosine monophosphate, PKA protein kinase A, DARPP-32 dopamine and cAMP-regulated phosphoprotein, 32 kDa, NAcc NAc core.

reported that mPFC provides its glutamatergic inputs to the NAc, and the IL preferentially projects to the NAcs and the PrL to the NAcc [47]. Therefore, we injected cre-dependent pAAV2/8-hSyn-DIO-hM4D(Gi)-mCherry (or pAAV2/8-hSyn-DIO-hM3D(Gq)-mCherry, pAAV2/8-hSyn-DIO-mCherry) bilaterally into the PrL region of the mPFC, along with a retrograde CaMKIIa promoter-driven pAAV2/Retro-CaMKIIa-EGFP-P2A-Cre-WPRE into bilateral NAcc of mice, allowing the selective targeting of glutamatergic neurons in the PrL. 5-d UMS was performed 15 days after virus injection. CNO was administered 30 min before behavioral experiments to selectively activate or inhibit the PrL-NAcc glutamatergic projections (Fig. 4a, b).

In the open field test, activation/inhibition of glutamatergic projections from the PrL to NAcc had no significant effect on the total distance moved, line crosses, rearing, or center entries (Fig. 4c–h). This suggests that PrL-NAcc glutamatergic projections have no role in locomotor activity after 5-d UMS. Next, we investigated the effects of activating/inhibiting PrL-NAcc glutamatergic projections on depression-like behavior after 5-d UMS using the forced swim test, sucrose preference test, and tail suspension test. In the forced swim test, the results showed that activation of PrL-NAcc glutamatergic projections reduced the duration of immobility (Fig. 4i) and increased the duration of swimming (Fig. 4k) in the forced swim test. However, inhibition of PrL-NAcc glutamatergic projections did not affect immobility or swimming in the forced swim test. Interestingly, activation of PrL-NAcc glutamatergic projections had no effect on the duration of climbing, while inhibition of PrL-NAcc glutamatergic projections decreased the duration of climbing (Fig. 4j). In the sucrose preference test, activation of PrL-NAcc glutamatergic projections increased sucrose preference (Fig. 4m). Finally, in the tail suspension test, activation of PrL-NAcc glutamatergic projections decreased immobility time (Fig. 4n).

Next, we investigated the effects of activating/inhibiting PrL-NAcc glutamatergic projections on the levels of RASD2-positive and DRD2-positive neurons in the NAcc by immunofluorescence. We found that activation of PrL-NAcc glutamatergic projections increased the co-expression of RASD2 and c-Fos in the NAcc, and inhibition of PrL-NAcc glutamatergic projections decreased that co-expression (Fig. 4o). Similarly, the activation of PrL-NAcc glutamatergic projections increased the co-expression of DRD2 and c-Fos in the NAcc, and inhibition of PrL-NAcc glutamatergic projections decreased that co-expression (Supplementary Fig. 2a, b).

Rasd2 overexpression in DRD2$^{\text{PrL-NAcc}}$ neurons alleviates depression-like behaviors after 5-d UMS

Our experiments have shown that 5-d UMS decreases the interaction of RASD2 and DRD2 in the NAc. *Rasd2* overexpression reduces depression-like behaviors after 5-d UMS while increasing the co-expression of RASD2 and DRD2 in the NAcc. However, it remains to be seen if RASD2 expression specifically in DRD2$^{\text{PrL-NAcc}}$ neurons underlies these effects on depression-like behavior. To address this question, *Drd2-cre* transgenic mice were used to construct mice with *Rasd2* overexpression selectively in DRD2$^{\text{PrL-NAcc}}$ neurons (Fig. 5a–c). We injected pAAV2/9-EF1a-fDIO-mCherry-P2A-3xFLAG-Rasd2-WPRE (0.4 μL, 7.10E + 12 V.G./mL, Obio Technology) in bilateral PrL and pAAV2/Retro-hSyn-DIO-EGFP-T2A-NLS-FLPO-WPRE (0.4 μL, 8.40E + 12 V.G./mL, Obio Technology) bilaterally in the NAcc of wild type and *Drd2-cre* mice. 15 days after the virus injection, mice received the 5-d UMS regimen. Co-localization of DRD2 and RASD2 in the NAcc was investigated by immunofluorescence, and we found that *Drd2-cre* mice had higher co-expression of RASD2 and DRD2 in the NAcc (Fig. 5d).

In the open field test, *Rasd2* overexpression in DRD2$^{\text{PrL-NAcc}}$ neurons had no significant effect on the total distance moved, line crosses, rearing, or center entries (Fig. 5e–j), suggesting that *Rasd2* overexpression in DRD2$^{\text{PrL-NAcc}}$ neurons had no effect on locomotor activity after 5-d UMS. In the forced swim test, *Rasd2* overexpression in DRD2$^{\text{PrL-NAcc}}$ neurons significantly reduced the duration of immobility (Fig. 5k), and significantly increased the duration of climbing and swimming (Fig. 5l, m). In addition, *Rasd2* overexpression in DRD2$^{\text{PrL-NAcc}}$ neurons increased sucrose preference (Fig. 5o) and reduced the duration of immobility in the tail suspension test (Fig. 5p).

DISCUSSION

The present study showed a regulatory mechanism of *Rasd2* expression on 5-d UMS-induced depression-like behavior. We found that *Rasd2* overexpression alleviated depression-like behaviors and activated the DRD2-cAMP-PKA-DARPP-32 signaling pathway. 5-d UMS inhibited PrL-to-NAcc projections, whereas further activation of the PrL-NAcc glutamatergic circuit by excitatory and inhibitory designer receptors exclusively activated by designer drugs (DREADDs) attenuated depression-like behavior and increased the activity of RASD2- and DRD2-positive neurons. Based on *Drd2-cre* transgenic mice, we demonstrated that *Rasd2* overexpression in DRD2$^{\text{PrL-NAcc}}$ neurons attenuated depression-like behaviors.

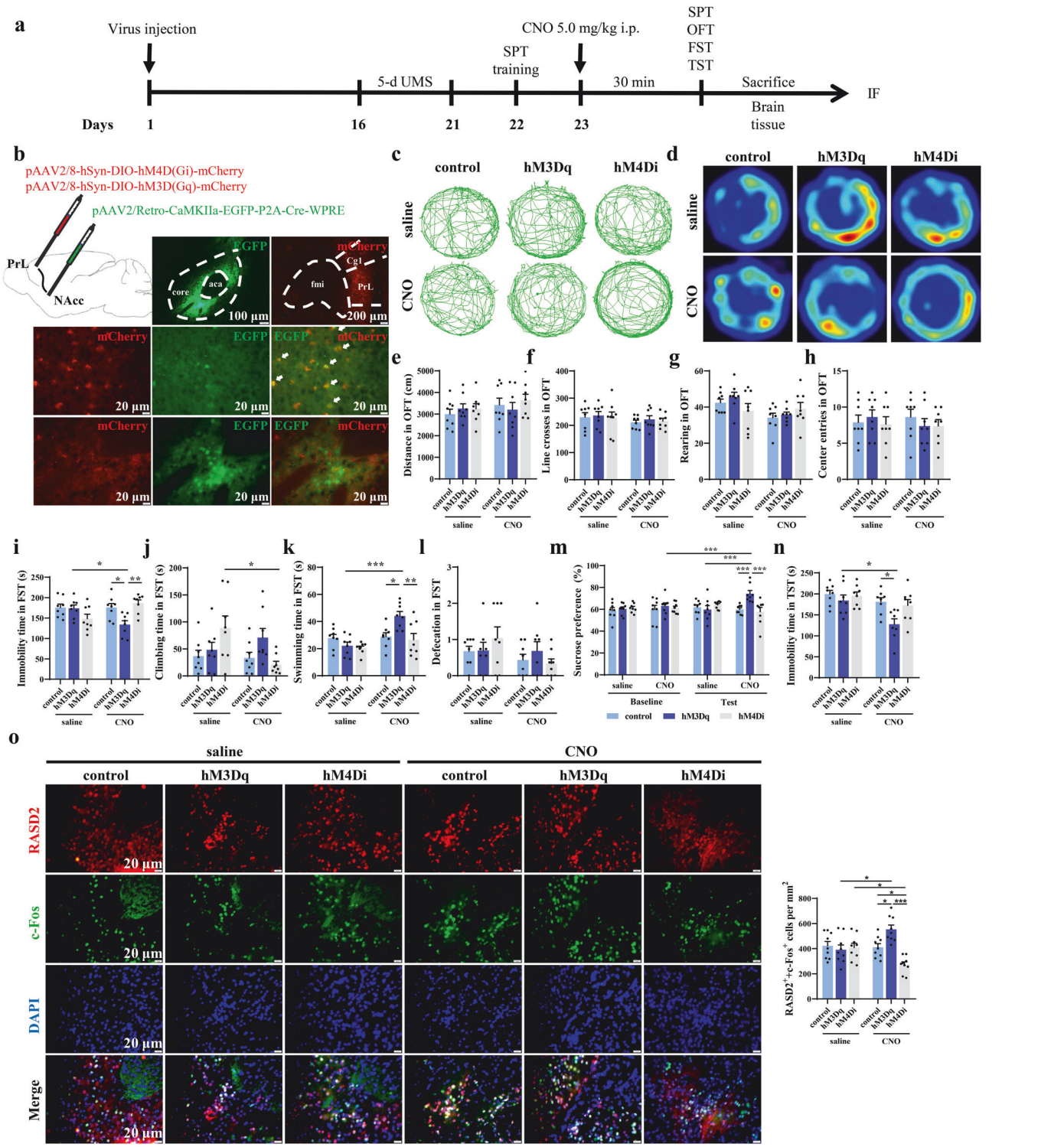

5-day repeated forced swim stress was shown to induce reduced sucrose preference in mice and this emotional symptom persisted for at least 4 weeks [48], however, the progressive increase in floating may reflect an adaptive learned behavioral response that promotes survival [49, 50]. In our studies, 5-d UMS experience was sufficient to induce depression-like behaviors in mice (including behavioral despair and anhedonia). In the forced swim test, 5-d UMS reduced the duration of climbing and swimming, as well as increased the duration of immobility. Catecholaminergic and serotonergic systems have differential roles in climbing and swimming behavior in the forced swim test, respectively [39, 40]. Therefore, depression-like behaviors induced by 5-d UMS may be related to changes in both catecholamine and serotonin systems. In addition, 5-d UMS increased serum corticosterone levels in mice and reduced the expression of c-Fos in the NAc (core and shell) and mPFC (Cg1, PrL, and IL), findings that are consistent with the previous studies [41, 42, 51, 52]. Together, these findings indicate that this 5-d UMS procedure produced a valid model of depression.

Fig. 4 Activation of the PrL-NAcc circuit attenuates depression-like behavior after 5-d UMS. a Schematic of experimental design and timeline. **b** Schematic diagram of microinjection of viral vectors into mouse PrL and NAcc sites (top, left); Representative images of CaMKIIa-cre injection site in NAcc (green) (top, middle) and hM4Di injection site in PrL (red) (top, right); Representative images of mCherry- (middle, left) and EGFP- (middle, middle) positive neurons in the PrL; Representative image of mCherry and EGFP co-labeled in the PrL (middle, right), arrows indicate co-expressed neurons; Representative images of mCherry- (bottom, left) and EGFP- (bottom, middle) positive neurons in the NAcc; Representative image of mCherry and EGFP co-labeled in the NAcc (bottom, right). Scale bar = 200 μm, 100 μm and 20 μm. Representative tracks (**c**) and heatmaps (**d**) displaying mouse movement in the open field test. Total distance moved (**e**), line crosses (**f**), rearing (**g**), and center entries (**h**) in the open field test. $N = 8$ mice for each group. Two-way ANOVA (factor 1: CNO; factor 2: virus): distance, $F_{CNO\times virus\ (2,\ 42)} = 0.4916$, $p = 0.6151$; $F_{virus\ (2,\ 42)} = 0.4595$, $p = 0.6347$; $F_{CNO\ (1,\ 42)} = 1.368$, $p = 0.2488$; line crosses, $F_{CNO\times virus\ (2,\ 42)} = 0.0273$, $p = 0.9731$; $F_{virus\ (2,\ 42)} = 0.2017$, $p = 0.8182$; $F_{CNO\ (1,\ 42)} = 1.571$, $p = 0.2170$; rearing, $F_{CNO\times virus\ (2,\ 42)} = 2.242$, $p = 0.1188$; $F_{virus\ (2,\ 42)} = 0.4293$, $p = 0.6538$; $F_{CNO\ (1,\ 42)} = 5.893$, $p = 0.0196$; center entries, $F_{CNO\times virus\ (2,\ 42)} = 0.4996$, $p = 0.6103$; $F_{virus\ (2,\ 42)} = 0.2914$, $p = 0.7487$; $F_{CNO\ (1,\ 42)} = 0.0937$, $p = 0.7611$. Duration of immobility (**i**), climbing (**j**), and swimming (**k**), and the number of fecal boli (defecation) (**l**) in the forced swim test. $N = 8$ mice for each group. Two-way ANOVA (factor 1: CNO; factor 2: virus): immobility, $F_{CNO\times virus\ (2,\ 42)} = 8.899$, $p = 0.0006$; $F_{virus\ (2,\ 42)} = 2.824$, $p = 0.0707$; $F_{CNO\ (1,\ 42)} = 0.0006$, $p = 0.9374$. Tukey's HSD post hoc test: in CNO-treated mice, $p_{(control\ vs.\ hM3Dq)} = 0.0287$, $p_{(hM3Dq\ vs.\ hM4Di)} = 0.0031$; in hM3Dq-treated mice, $p_{(saline\ vs.\ CNO)} = 0.0414$; climbing, $F_{CNO\times virus\ (2,\ 42)} = 5.285$, $p = 0.0090$; $F_{virus\ (2,\ 42)} = 1.645$, $p = 0.2052$; $F_{CNO\ (1,\ 42)} = 1.917$, $p = 0.1735$. Tukey's HSD post hoc test: in hM4Di-treated mice, $p_{(saline\ vs.\ CNO)} = 0.0199$; swimming, $F_{CNO\times virus\ (2,\ 42)} = 6.231$, $p = 0.0043$; $F_{virus\ (2,\ 42)} = 4.903$, $p = 0.0122$; $F_{CNO\ (1,\ 42)} = 14.91$, $p = 0.0004$. Tukey's HSD post hoc test: in CNO-treated mice, $p_{(control\ vs.\ hM3Dq)} = 0.0137$, $p_{(hM3Dq\ vs.\ hM4Di)} = 0.0030$; in hM3Dq-treated mice, $p_{(saline\ vs.\ CNO)} = 0.0001$; defecation, $F_{CNO\times virus\ (2,\ 42)} = 1.371$, $p = 0.2650$; $F_{virus\ (2,\ 42)} = 0.2623$, $p = 0.7705$; $F_{CNO\ (1,\ 42)} = 3.382$, $p = 0.0730$. **m** Graph represents sucrose preference (%) before (Day 0) and after (Day 23) treatment. $N = 8$ mice for each group. Three-way ANOVA (factor 1: CNO; factor 2: virus; factor 3: time): $F_{CNO\times virus\times time\ (2,\ 84)} = 5.077$, $p = 0.008$; $F_{time\times virus\ (2,\ 84)} = 2.096$, $p = 0.129$; $F_{time\times CNO\ (1,\ 84)} = 0.426$, $p = 0.516$; $F_{CNO\times virus\ (2,\ 84)} = 4.261$, $p = 0.017$; $F_{virus\ (2,\ 84)} = 2.101$, $p = 0.129$; $F_{CNO\ (1,\ 84)} = 0.537$, $p = 0.466$; $F_{time\ (1,\ 84)} = 3.529$, $p = 0.064$. Tukey's HSD post hoc test: in CNO + hM3Dq-treated mice, $p_{(baseline\ vs.\ treatment)} < 0.001$; after treatment: in CNO-treated mice, $p_{(control\ vs.\ hM3Dq)} < 0.001$, $p_{(hM3Dq\ vs.\ hM4Di)} < 0.001$; in hM3Dq-treated mice, $p_{(saline\ vs.\ CNO)} < 0.001$. **n** Duration of immobility in the tail suspension test. $N = 8$ mice for each group. Two-way ANOVA (factor 1: CNO; factor 2: virus): $F_{CNO\times virus\ (2,\ 42)} = 1.706$, $p = 0.1940$; $F_{virus\ (2,\ 42)} = 5.142$, $p = 0.0101$; $F_{CNO\ (1,\ 42)} = 5.142$, $p = 0.0011$. Tukey's HSD post hoc test: in CNO-treated mice, $p_{(control\ vs.\ hM3Dq)} = 0.0212$; in hM3Dq-treated mice, $p_{(saline\ vs.\ CNO)} = 0.0128$. **o** Effects of PrL-NAcc circuit activation/inhibition on the activity of RASD2-positive neurons in the NAcc after 5-d UMS (scale bar, 20 μm). Two-way ANOVA (factor 1: CNO; factor 2: virus): $F_{CNO\times virus\ (2,\ 48)} = 10.92$, $p = 0.0001$; $F_{virus\ (2,\ 48)} = 8.605$, $p = 0.0006$; $F_{CNO\ (1,\ 48)} = 0.03595$, $p = 0.8504$. $N = 3$ mice per group. Tukey's HSD post hoc test: in CNO-treated mice, $p_{(control\ vs.\ hM3Dq)} = 0.0329$, $p_{(control\ vs.\ hM4Di)} = 0.0379$, $p_{(hM3Dq\ vs.\ hM4Di)} < 0.0001$; in hM3Dq-treated mice, $p_{(saline\ vs.\ CNO)} = 0.0100$; in hM4Di-treated mice, $p_{(saline\ vs.\ CNO)} = 0.0450$. The data are expressed as mean ± s.e.m. $^*p < 0.05$, $^{**}p < 0.01$ and $^{***}p < 0.001$. 5-d UMS 5-day unpredictable mild stress, OFT open field test, FST forced swim test, TST tail suspension test, IF immunofluorescence, CNO clozapine-N-oxide, DRD2 dopamine D2 receptor, NAcc NAc core, Cg1 cingulate cortex 1, PrL prelimbic cortex, IL infralimbic cortex.

Based on the previous studies showing that stress alters the expression of *Rasd2* in the mPFC [15, 16], we examined changes in RASD2 levels in brain regions of mice after 5-d UMS. Both immunohistochemistry and western blotting data showed that 5-d UMS reduced the expression of RASD2 in the NAc and mPFC. Stress-induced changes in the expression of DRD1 and DRD2 are related to the type [53, 54], and duration [3, 55–58] of stress. Resistant rats exposed to chronic mild stress for both 2 and 5 weeks showed DRD2 downregulation in the NAc core [58]. DRD2 density was down-regulated after 2 weeks of chronic mild stress, but no changes in DRD2 biosynthesis (i.e. *Drd2* mRNA levels) were observed. However, 5 weeks of chronic mild stress produced different effects, resistant rats showed strong neuroplasticity by regulating DRD2 density and *Drd2* mRNA levels [58]. These alterations buffer the effects of stress and control the normalization of mesolimbic dopamine circuits in stress-resistant animals by enhancing DRD2 biosynthesis [3, 58], and stress-reactive rats may exhibit a delayed DRD2 response to stress compared to stress-resistant animals, resulting in an anhedonia behavior [58]. In addition, stress type also has different effects on the expression of DRD1 and DRD2. Chronic restraint stress (1 h/ day for 12 days) induced a decrease in DRD1 density in the NAc, but did not affect DRD2 density. Chronic immobilization stress (2 h/day for 10 days) induced an increase in DRD2 ligand binding level in rats NAc shell [57]. Mice exposed to chronic restraint stress (6 h/day for 21 consecutive days) showed a decrease in the level of *Drd1* mRNA in the NAc [54]. In addition, maternal deprivation (6 h/ day for 14 days) combined with chronic unpredictable stress (21 days) reduced the expression of DRD1 and DRD2 in the NAc [53], however, 16 consecutive days of chronic unpredictable stress induced an increase in the expression of DRD1 in rats' limbic system [56]. In our data, 5-d UMS increased the protein expression of DRD1 and decreased the expression of DRD2 in the NAc. In addition, 5-d UMS had no significant effect on the expression of DRD1 and DRD2 proteins in the mPFC, this is consistent with previous studies in which there were no change in DRD1 and DRD2 expression in the PFC of mice exposed to chronic immobilization stress or chronic social defeat [54, 59]. It has been pointed out that stress may increase extracellular dopamine levels in the limbic structures, but this may be offset by the opposing effects imposed by the hypodopaminergic functioning of the mPFC [59–61].

DARPP-32 is a cytoplasmic protein that plays a central role in regulating dopamine signaling [62]. Upon PKA-catalyzed phosphorylation of the DARPP-32 Thr34 site, DARPP-32 is converted to an inhibitor of PP-1 [63]. Inhibition of PP-1 prevents the dephosphorylation of target proteins regulated by PKA, thereby enhancing cAMP-mediated signaling [64]. In the present study, 5-d UMS significantly increased DARPP-32 expression in both NAc and mPFC. In addition, 5-d UMS significantly reduced GluA1 expression in the mPFC, which is consistent with previous studies [6, 65]. The changes in GluA1 expression in the mPFC suggest that glutamatergic neurons in the mPFC may be involved in the mechanism of 5-d UMS exposure that induced depression-like behaviors.

PFC preferentially projects to the NAcc, and the vHipp preferentially projects to the NAcs [25, 46]. To explore the effect of 5-d UMS on the projections of subregions of the mPFC to the NAcc, we injected the retrograde tracer Fluorogold into the NAcc and found Fluorogold-positive neurons expressed in all three subregions of the mPFC (Cg1, PrL, and IL), indicating that Cg1, PrL, and IL project to NAcc. However, 5-d UMS only reduced c-Fos expression in Fluorogold-positive neurons in the PrL, suggesting that 5-d UMS inhibited the PrL-NAcc circuit. It has been found that chronic stress significantly reduced the firing rate of PrL neurons [66], and stress-induced behavioral deficits were mediated partly by molecular adaptations in the PrL via cortical projections to distinct subcortical targets [67]. Therefore, in further study, we focused on PrL projections to NAcc on depression-like behavior.

To further evaluate the role of this circuit in 5-d UMS, we constructed mice with overexpression or reduced expression of *Rasd2* in the NAcc by regional microinjection of lentivirus vectors. The results showed that *Rasd2* overexpression reduced 5-d UMS-induced anhedonia and other depression-like behaviors while reduced expression was without effect. In the forced swim test, *Rasd2* overexpression significantly reduced the duration of

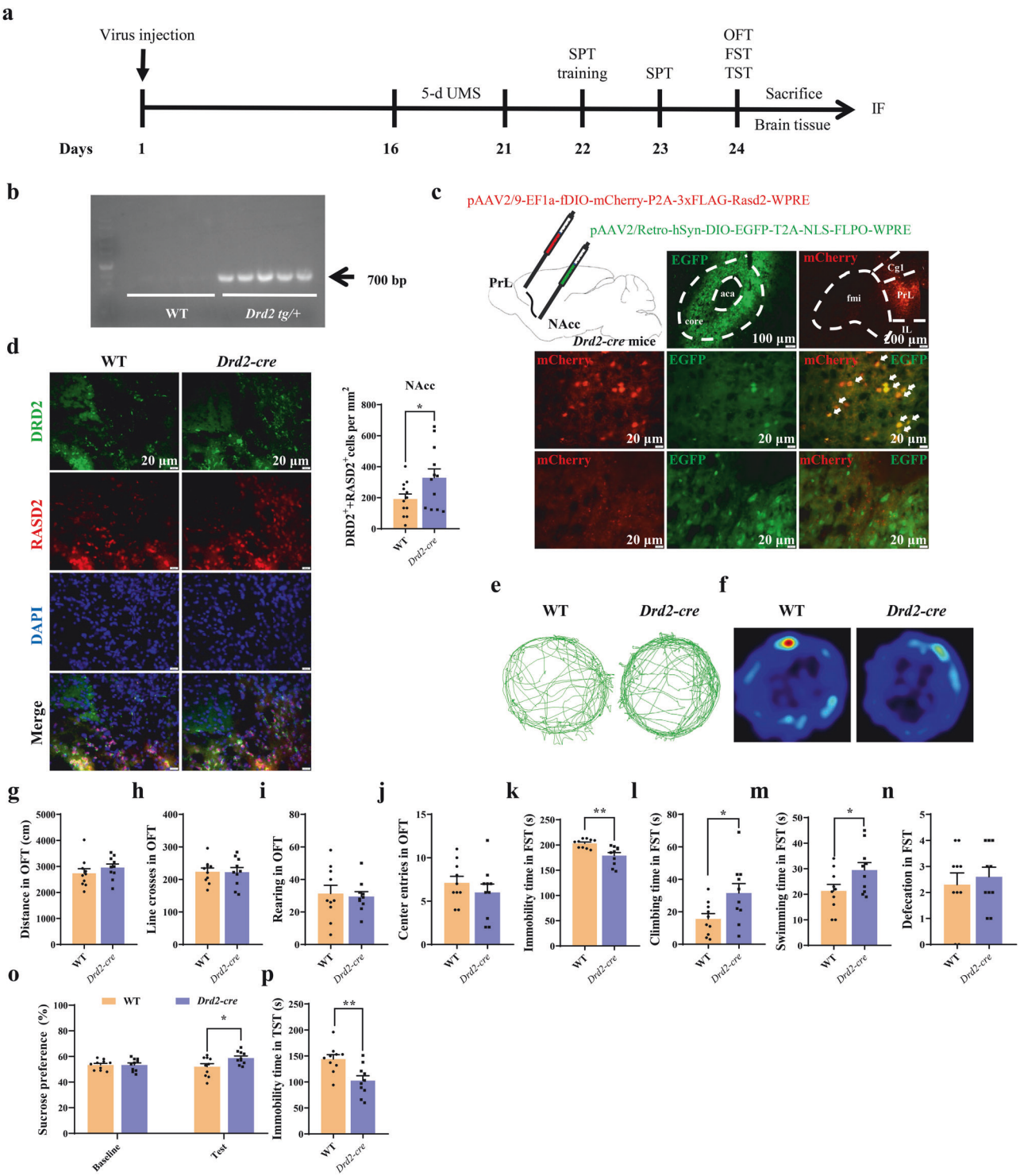

climbing and increased the duration of swimming after 5-d UMS. Climbing scores in the forced swim test and other antidepressant-like effects depend directly on the balance of DRD2 and DRD1 activity [68–71]. Higher climbing scores in the forced swim test are observed after administration of the DRD2 antagonist raclopride, which appears to increase dopamine stimulation of DRD1 [68]. Rats treated with high doses of raclopride, exhibit immobility or climbing most of the time, as if they are constantly trying to leave the device and only taking short breaks in their efforts to escape [69]. Based on these findings, we inferred that the role of *Rasd2* overexpression (reduced depression-like behaviors, but without increasing climbing time) on antidepressant-like effects may be related to DRD2 expression.

DRD1 couples to $G\alpha_s$ and $G\alpha_{olf}$ G protein subunits, through which dopamine increases adenylate cyclase activity, increases cAMP production, and activates PKA [72]. In contrast, DRD2 couples to $G\alpha_i$ and $G\alpha_o$ G protein subunits, through which dopamine decreases cAMP and decreases PKA activity [72]. One of the main targets of PKA is DARPP-32, which is highly expressed in dopamine-responsive striatal neurons and plays a key role in the regulation of downstream signaling transduction pathways [73, 74]. We found that *Rasd2* overexpression activated the

Fig. 5 *Rasd2* overexpression in DRD2$^{PrL\text{-}NAcc}$ neurons decreases depression-like behavior. a Schematic of experimental design and timeline. **b** Representative image for the identification of *Drd2-cre* genotypes. **c** Schematic diagram of microinjection of viral vectors into mouse PrL and NAcc sites (top, left); Representative images of EGFP (top, middle) and fDIO-mCherry (top, right) injection sites in the NAcc and PrL, respectively; Representative images of mCherry- (middle, left) and EGFP- (middle, middle) positive neurons in the PrL; Representative image of mCherry and EGFP co-labeled in the PrL (middle, right), arrows indicate co-expressed neurons.; Representative images of mCherry- (bottom, left) and EGFP- (bottom, middle) positive neurons in the NAcc; Representative image of mCherry and EGFP co-labeled in the NAcc (bottom, right). **d** Representative images showing co-localization of RASD2 and DRD2 in NAcc 3 weeks after virus injection (left, scale bar = 20 μm) and the number of DRD2-positive neurons that co-express RASD2 in NAcc (Right). $N = 4$ mice per group. Two-tailed unpaired *t*-test: $t_{(22)} = 2.101$, $p = 0.0474$. Representative tracks (**e**) and heatmaps (**f**) displaying mouse movement in the open field test. Total distance moved (**g**), line crosses (**h**), rearing (**i**), and center entries (**j**) in the open field test. $N = 10$ mice per group. Two-tailed unpaired *t*-test: distance, $t_{(18)} = 0.9870$, $p = 0.3367$; line crosses, $t_{(18)} = 0.0605$, $p = 0.9524$; rearing, $t_{(18)} = 0.3031$, $p = 0.7653$; center entries, $t_{(18)} = 0.8985$, $p = 0.3808$. Duration of immobility (**k**), climbing (**l**), and swimming (**m**), and the number of fecal boli (defecation) (**n**) in the forced swim test. $N = 10$ mice per group. Two-tailed unpaired *t*-test: immobility, $t_{(18)} = 3.658$, $p = 0.0018$; climbing, $t_{(18)} = 2.384$, $p = 0.0284$; swimming, $t_{(18)} = 2.115$, $p = 0.0486$; defecation, $t_{(18)} = 0.5153$, $p = 0.6128$. **o** Graph represents sucrose preference (%) before (Day 0) and after (Day 23) treatment. $N = 10$ mice for each group. Two-way ANOVA (factor 1: time; factor 2: treatment): $F_{time \times treatment\ (1,\ 36)} = 3.817$, $p = 0.0586$; $F_{time\ (1,\ 36)} = 1.321$, $p = 0.2581$; $F_{treatment\ (1,36)} = 3.817$, $p = 0.0586$. Tukey's HSD post hoc test: after treatment, $p_{(WT\ vs.\ Drd2\text{-}cre)} = 0.0426$. **p** Duration of immobility in the tail suspension test. $N = 10$ mice per group. Two-tailed unpaired *t*-test: $t_{(18)} = 3.300$, $p = 0.0040$. The data are expressed as mean ± s.e.m. $^*p < 0.05$. 5-d UMS 5-day unpredictable mild stress, OFT open field test, FST forced swim test, TST tail suspension test, IF immunofluorescence, WT wild type, Cg1 cingulate cortex 1, PrL prelimbic cortex, IL infralimbic cortex, NAcc NAc core, DRD2 dopamine D2 receptor.

DRD2-cAMP-PKA-DARPP-32 signaling pathway (but not DRD1) in the NAc. Consistent with this hypothesis, 5-d UMS increased the interaction between DRD2 and RASD2 in the NAc, and *Rasd2* overexpression increased the colocalization of DRD2 and RASD2 in the NAcc. These results suggest that the effects of RASD2 that alleviate depression-like behaviors after 5-d UMS are mediated by DRD2-containing neurons.

The PFC-NAc circuit is thought to be critical for goal-directed behavior and reward processes [74, 75]. PFC modulates NAc neuronal activity by sending direct excitatory inputs to GABAergic NAc neurons [76–79]. Clinical study has found that increases in NAc-PFC connectivity correlate with reduced symptom severity in selective serotonin reuptake inhibitor-responsive patients with depression [80]. NAc output to PFC was much weaker than the inputs from PFC to NAc [81, 82]. In the present study, 5-d UMS reduced RASD2 expression in the NAc and decreased GluA1 expression in the mPFC. And *Rasd2* overexpression in the NAcc increased GluA1 expression in the mPFC. It has been found that blocking neurotransmission in NAc D2-MSNs was able to alter mPFC expression of genes (such as *Drd1, Drd2, ADORA2A*) [83]. The α-amino-3-hydroxy-5-methyl-4-isoxazolepropionic acid (AMPA) receptor (GluA1-4) is enriched in dopamine-innervated regions, including the mPFC [84, 85]. Both DRD1 and DRD2 upregulate GluA1 phosphorylation in mPFC neurons via a direct and indirect mechanism, respectively [85]. In our data, RASD2 interacts with DRD2, and *Rasd2* overexpression increased the co-labeling of RASD2 and DRD2 and decreased the expression of the MSN marker DARPP-32 in the NAcc. Therefore, we speculate that *Rasd2* overexpression in the NAcc may affect GluA1 expression in the mPFC by regulating D2-MSNs activity. Therefore, both in human and animal models, are required to elucidate the exact mechanisms by which interactions between the NAc and PFC, as well as to clarify the role played by *Rasd2* in the circuit in further study.

Studies have shown that PrL sends excitatory glutaminergic inputs directly to NAc D2-MSNs [86, 87], and these PFC neurons are CaMKIIa-positive [25]. To further evaluate the role of RASD2 in PrL-NAcc glutaminergic projections in depression-like behavior, activation and inhibition of this circuit with DREADDs was used G_q-DREADD activation of the PrL-NAcc glutaminergic projections alleviated depression-like behaviors, including anhedonia and behavioral despair, although there was no change in the duration of climbing in the forced swim test. G_i-DREADD inhibition of the PrL-NAcc glutaminergic projections reduced the duration of climbing in the forced swim test, suggesting that inhibition of PrL-NAcc glutaminergic projections may have effects on DRD1-containing circuits, which needs to be further explored. Immunofluorescence results showed that activation or inhibition of PrL-NAcc glutaminergic projections increased or decreased activation of RASD2-positive neurons and DRD2-positive neurons in the NAcc, respectively. These results confirmed that the activation of PrL-NAcc glutaminergic projections alleviates depression-like behaviors (such as anhedonia and behavioral despair) in 5-d UMS mice, and these effects are related to the activation of RASD2- and DRD2-positive neurons in the NAcc.

Approximately 35%-50% of CaMKIIα neurons were positive for DRD2, and approximately 85% of DRD2 were co-labeled with CaMKIIα (the neuronal marker for pyramidal neurons) in all layers of PrL [88]. DRD2 in the mPFC regulates the synaptic transmission of PrL$^{NAc\text{-}projecting}$ neurons [88], in addition, PrL sends glutaminergic inputs directly to NAc D2-MSNs [86, 87]. In our study, we found that the PrL-NAcc glutamatergic circuit modulated depression-like behaviors as well as the expression level of DRD2- and RASD2-positive neurons in the NAcc. Combined with our previous results that there was an interaction between RASD2 and DRD2 and 5-d UMS reduced RASD2 expression in the mPFC. we speculated that the expression of *Rasd2* in DRD2$^{NAcc\text{-}projecting}$ neurons in the PrL might have an effect on depression-like behavior. Therefore, we constructed mice that selectively overexpress *Rasd2* in DRD2$^{PrL\text{-}NAcc}$ neurons, and subsequently explored changes in depression-like behaviors and the co-expression of DRD2 and RASD2 in the NAcc. Our data showed that *Rasd2* overexpression in DRD2$^{PrL\text{-}NAcc}$ neurons alleviated depression-like behaviors (decreased anhedonia and behavioral despair, increased the duration of climbing and swimming in the forced swim test) in 5-d UMS mice, and increased co-expression of RASD2 and DRD2 in the NAcc. DRD2 had a cell type-specific role in the mPFC to regulate social behavior, which may be mediated by the mPFC-to-NAc pathway [88]. However, further experiments are still needed to verify whether DRD2 is expressed in pyramidal neurons of PrL and whether DRD2 is expressed in the MSNs of NAcc.

Markedly, the following limitations existed in the current study. We have only demonstrated that the 5-d UMS paradigm induces depression-like behaviors and that this effect can be observed in 2-3 days after the paradigm, but how long the observed phenotypes can last, and whether *Rasd2* has the same effects on mice exposed to longer periods of chronic unpredictable mild stress still requires further study. And whether differences in *Rasd2*/RASD2 expression in the NAc can be considered as a biological marker for depression diagnosis needs to be addressed in clinical studies. In addition, we chose the CaMKIIa promoter to selectively target glutamatergic neurons in the PrL region of the mPFC, although CaMKIIa is usually considered an excitatory neuron-specific promoter, some GABAergic projection neurons also express CaMKIIa [89]. Hence, the precise target of these subpopulations could be more necessary.

In totality, the present findings demonstrate a critical role for RASD2 in the regulation of depression-like behaviors in the PrL-NAcc circuit and modulation of PrL-NAcc projections by DRD2-containing neurons. These results provide substantial evidence for a new potential molecular target for the development of a treatment for depression, as well as a theoretical basis for precision medicine treatment of depression.

DATA AVAILABILITY

Data are available from the corresponding author upon reasonable request.

REFERENCES

1. World Health Organization. Depression and other common mental disorders: Global Health Estimates. WHO Document Production Services: Geneva, 2017.
2. Lancet T. Ensuring care for people with depression. Lancet. 2022;399:885.
3. Dziedzicka-Wasylewska M, Solich J, Korlatowicz A, Faron-Górecka A. What do the animal studies of stress resilience teach us. Cells. 2021;10:1630.
4. Wang H, Cui W, Chen W, Liu F, Dong Z, Xing G, et al. The laterodorsal tegmentum-ventral tegmental area circuit controls depression-like behaviors by activating ErbB4 in DA neurons. Mol Psychiatry. 2023;28:1027–45.
5. Bogdan R, Pizzagalli DA. Acute stress reduces reward responsiveness: implications for depression. Biol Psychiatry. 2006;60:1147–54.
6. Cooper JA, Nuutinen MR, Lawlor VM, DeVries B, Barrick EM, Hossein S, et al. Reduced adaptation of glutamatergic stress response is associated with pessimistic expectations in depression. Nat Commun. 2021;12:3166.
7. Ossewaarde L, Qin S, Van Marle HJ, van Wingen GA, Fernández G, Hermans EJ. Stress-induced reduction in reward-related prefrontal cortex function. Neuroimage. 2011;55:345–52.
8. Porcelli AJ, Lewis AH, Delgado MR. Acute stress influences neural circuits of reward processing. Front Neurosci. 2012;6:157.
9. Nusslock R, Alloy LB. Reward processing and mood-related symptoms: an RDoC and translational neuroscience perspective. J Affect Disord. 2017;216:3–16.
10. Alloy LB, Chat IK, Grehl MM, Stephenson AR, Adogli ZV, Olino TM, et al. Reward and immune systems in emotion (RISE) prospective longitudinal study: protocol overview of an integrative reward-inflammation model of first onset of major depression in adolescence. Brain Behav Immun Health. 2023;30:100643.
11. Baik JH. Stress and the dopaminergic reward system. Exp Mol Med. 2020;52:1879–90.
12. Bourne HR, Sanders DA, McCormick F. The GTPase superfamily: conserved structure and molecular mechanism. Nature. 1991;349:117–27.
13. Vargiu P, De Abajo R, Garcia-Ranea JA, Valencia A, Santisteban P, Crespo P, et al. The small GTP-binding protein, Rhes, regulates signal transduction from G protein-coupled receptors. Oncogene. 2004;23:559–68.
14. Napolitano F, D'Angelo L, de Girolamo P, Avallone L, de Lange P, Usiello A. The thyroid hormone-target gene rhes a novel crossroad for neurological and psychiatric disorders: new insights from animal models. Neuroscience. 2018;384:419–28.
15. Lisowski P, Wieczorek M, Goscik J, Juszczak GR, Stankiewicz AM, Zwierzchowski L, et al. Effects of chronic stress on prefrontal cortex transcriptome in mice displaying different genetic backgrounds. J Mol Neurosci. 2013;50:33–57.
16. Cheng Z, Zhao F, Piao J, Cui R, Li B. Rasd2 mediates acute fasting-induced antidepressant-like effects via dopamine D2 receptor activation in ovariectomized mice. Int J Neuropsychopharmacol. 2023;26:217–29.
17. Errico F, Santini E, Migliarini S, Borgkvist A, Centonze D, Nasti V, et al. The GTP-binding protein Rhes modulates dopamine signalling in striatal medium spiny neurons. Mol Cell Neurosci. 2008;37:335–45.
18. Ghiglieri V, Napolitano F, Pelosi B, Schepisi C, Migliarini S, Di Maio A, et al. Rhes influences striatal cAMP/PKA-dependent signaling and synaptic plasticity in a gender-sensitive fashion. Sci Rep. 2015;5:10933.
19. Vitucci D, Di Giorgio A, Napolitano F, Pelosi B, Blasi G, Errico F, et al. Rasd2 modulates prefronto-striatal phenotypes in humans and 'schizophrenia-like behaviors' in mice. Neuropsychopharmacology. 2016;41:916–27.
20. Antoniuk S, Bijata M, Ponimaskin E, Wlodarczyk J. Chronic unpredictable mild stress for modeling depression in rodents: meta-analysis of model reliability. Neurosci Biobehav Rev. 2019;99:101–16.
21. Franklin KBJ, Paxinos GF. Paxinos and Franklin's the mouse brain in stereotaxic coordinates, 4th ed. Amsterdam: Academic Press, an imprint of Elsevier; 2013.
22. Francis TC, Gaynor A, Chandra R, Fox ME, Lobo MK. The selective RhoA inhibitor Rhosin promotes stress resiliency through enhancing D1-medium spiny neuron plasticity and reducing hyperexcitability. Biol Psychiatry. 2019;85:1001–10.
23. Francis TC, Yano H, Demarest TG, Shen H, Bonci A. High-frequency activation of nucleus accumbens D1-MSNs drives excitatory potentiation on D2-MSNs. Neuron. 2019;103:432–44.e3.
24. Adrover MF, Shin JH, Quiroz C, Ferré S, Lemos JC, Alvarez VA. Prefrontal cortex-driven dopamine signals in the striatum show unique spatial and pharmacological properties. J Neurosci. 2020;40:7510–22.
25. Deroche MA, Lassalle O, Castell L, Valjent E, Manzoni OJ. Cell-type- and endocannabinoid-specific synapse connectivity in the adult nucleus accumbens core. J Neurosci. 2020;40:1028–41.
26. Cheng Z, Yang W, Li B, Cui R. KLF4 exerts sedative effects in pentobarbital-treated mice. J Mol Neurosci. 2021;71:596–606.
27. Dong Y, Zhou Y, Chu X, Chen S, Chen L, Yang B, et al. Dental noise exposed mice display depressive-like phenotypes. Mol Brain. 2016;9:50.
28. Shen CJ, Zheng D, Li KX, Yang JM, Pan HQ, Yu XD, et al. Cannabinoid CB(1) receptors in the amygdalar cholecystokinin glutamatergic afferents to nucleus accumbens modulate depressive-like behavior. Nat Med. 2019;25:337–49.
29. He ZX, Yin YY, Xi K, Xing ZK, Cao JB, Liu TY, et al. Nucleus accumbens Tac1-expressing neurons mediate stress-induced anhedonia-like behavior in mice. Cell Rep. 2020;33:108343.
30. Ma H, Li C, Wang J, Zhang X, Li M, Zhang R, et al. Amygdala-hippocampal innervation modulates stress-induced depressive-like behaviors through AMPA receptors. Proc Natl Acad Sci USA. 2021;118:e2019409118.
31. Grossman YS, Fillinger C, Manganaro A, Voren G, Waldman R, Zou T, et al. Structure and function differences in the prelimbic cortex to basolateral amygdala circuit mediate trait vulnerability in a novel model of acute social defeat stress in male mice. Neuropsychopharmacology. 2022;47:788–99.
32. Cheng ZQ, Fan J, Zhao FY, Su JY, Sun QH, Cui RJ, et al. Fasting produces antidepressant-like effects via activating mammalian target of rapamycin complex 1 signaling pathway in ovariectomized mice. Neural Regen Res. 2023;18:2075–81.
33. Cryan JF, Markou A, Lucki I. Assessing antidepressant activity in rodents: recent developments and future needs. Trends Pharmacol Sci. 2002;23:238–45.
34. Zhang D, Shen Q, Wu X, Xing D. Photobiomodulation therapy ameliorates glutamatergic dysfunction in mice with chronic unpredictable mild stress-induced depression. Oxid Med Cell Longev. 2021;2021:6678276.
35. Kim HD, Wei J, Call T, Quintus NT, Summers AJ, Carotenuto S, et al. Shisa6 mediates cell-type specific regulation of depression in the nucleus accumbens. Mol Psychiatry. 2021;26:7316–27.
36. Wager-Miller J, Murphy Green M, Shafique H, Mackie K. Collection of frozen rodent brain regions for downstream analyses. J Vis Exp. 2020;158:e60474.
37. Pandya CD, Hoda N, Crider A, Peter D, Kutiyanawalla A, Kumar S, et al. Transglutaminase 2 overexpression induces depressive-like behavior and impaired TrkB signaling in mice. Mol Psychiatry. 2017;22:745–53.
38. Yu H, Chen L, Lei H, Pi G, Xiong R, Jiang T, et al. Infralimbic medial prefrontal cortex signalling to calbindin 1 positive neurons in posterior basolateral amygdala suppresses anxiety- and depression-like behaviours. Nat Commun. 2022;13:5462.
39. Cryan JF, Page ME, Lucki I. Differential behavioral effects of the antidepressants reboxetine, fluoxetine, and moclobemide in a modified forced swim test following chronic treatment. Psychopharmacology. 2005;182:335–44.
40. Slattery DA, Cryan JF. Using the rat forced swim test to assess antidepressant-like activity in rodents. Nat Protoc. 2012;7:1009–14.
41. Brás JP, Guillot de Suduiraut I, Zanoletti O, Monari S, Meijer M, Grosse J, et al. Stress-induced depressive-like behavior in male rats is associated with microglial activation and inflammation dysregulation in the hippocampus in adulthood. Brain Behav Immun. 2022;99:397–408.
42. Yao C, Zhang Y, Sun X, Pei H, Wei S, Wang M, et al. Areca catechu L. ameliorates chronic unpredictable mild stress-induced depression behavior in rats by the promotion of the BDNF signaling pathway. Biomed Pharmacother. 2023;164:114459.
43. Dunlop BW, Nemeroff CB. The role of dopamine in the pathophysiology of depression. Arch Gen Psychiatry. 2007;64:327–37.
44. Surmeier DJ, Ding J, Day M, Wang Z, Shen W. D1 and D2 dopamine-receptor modulation of striatal glutamatergic signaling in striatal medium spiny neurons. Trends Neurosci. 2007;30:228–35.
45. Belujon P, Grace AA. Dopamine system dysregulation in major depressive disorders. Int J Neuropsychopharmacol. 2017;20:1036–46.
46. Li Z, Chen Z, Fan G, Li A, Yuan J, Xu T. Cell-type-specific afferent innervation of the nucleus accumbens core and shell. Front Neuroanat. 2018;12:84.
47. Ma YY, Lee BR, Wang X, Guo C, Liu L, Cui R, et al. Bidirectional modulation of incubation of cocaine craving by silent synapse-based remodeling of prefrontal cortex to accumbens projections. Neuron. 2014;83:1453–67.
48. Serchov T, Clement HW, Schwarz MK, Iasevoli F, Tosh DK, Idzko M, et al. Increased signaling via adenosine A1 receptors, sleep deprivation, imipramine, and ketamine inhibit depressive-like behavior via induction of Homer1a. Neuron. 2015;87:549–62.
49. Molendijk ML, de Kloet ER. Immobility in the forced swim test is adaptive and does not reflect depression. Psychoneuroendocrinology. 2015;62:389–91.

50. Mul JD, Zheng J, Goodyear LJ. Validity assessment of 5 day repeated forced-swim stress to model human depression in young-adult C57BL/6J and BALB/cJ mice. eNeuro. 2016;3:ENEURO.0201-0216.2016.
51. Grippo AJ, Na ES, Johnson RF, Beltz TG, Johnson AK. Sucrose ingestion elicits reduced Fos expression in the nucleus accumbens of anhedonic rats. Brain Res. 2004;1019:259–64.
52. Papp M, Gruca P, Lason M, Litwa E, Solecki W, Willner P. Optogenetic stimulation of medial prefrontal cortex excites GABAergic cells in the nucleus accumbens and hippocampus of Wistar-Kyoto rats exposed to chronic mild stress. Psychopharmacology. 2022;239:2299–307.
53. Zhang Y, Zhu X, Bai M, Zhang L, Xue L, Yi J. Maternal deprivation enhances behavioral vulnerability to stress associated with miR-504 expression in nucleus accumbens of rats. PLoS ONE. 2013;8:e69934.
54. Cao G, Meng G, Zhu L, Zhu J, Dong N, Zhou X, et al. Susceptibility to chronic immobilization stress-induced depressive-like behaviour in middle-aged female mice and accompanying changes in dopamine D1 and GABA(A) receptors in related brain regions. Behav Brain Funct. 2021;17:2.
55. Giardino L, Zanni M, Pozza M, Bettelli C, Covelli V. Dopamine receptors in the striatum of rats exposed to repeated restraint stress and alprazolam treatment. Eur J Pharmacol. 1998;344:143–7.
56. Ossowska G, Nowa G, Kata R, Klenk-Majewska B, Danilczuk Z, Zebrowska-Lupina I. Brain monoamine receptors in a chronic unpredictable stress model in rats. J Neural Transm. 2001;108:311–9.
57. Lucas LR, Wang CJ, McCall TJ, McEwen BS. Effects of immobilization stress on neurochemical markers in the motivational system of the male rat. Brain Res. 2007;1155:108–15.
58. Zurawek D, Faron-Gorecka A, Kusmider M, Kolasa M, Gruca P, Papp M, et al. Mesolimbic dopamine D_2 receptor plasticity contributes to stress resilience in rats subjected to chronic mild stress. Psychopharmacology. 2013;227:583–93.
59. Jin HM, Shrestha Muna S, Bagalkot TR, Cui Y, Yadav BK, Chung YC. The effects of social defeat on behavior and dopaminergic markers in mice. Neuroscience. 2015;288:167–77.
60. Carter CJ, Pycock CJ. Behavioural and biochemical effects of dopamine and noradrenaline depletion within the medial prefrontal cortex of the rat. Brain Res. 1980;192:163–76.
61. Scornaiencki R, Cantrup R, Rushlow WJ, Rajakumar N. Prefrontal cortical D1 dopamine receptors modulate subcortical D2 dopamine receptor-mediated stress responsiveness. Int J Neuropsychopharmacol. 2009;12:1195–208.
62. Svenningsson P, Tzavara ET, Witkin JM, Fienberg AA, Nomikos GG, Greengard P. Involvement of striatal and extrastriatal DARPP-32 in biochemical and behavioral effects of fluoxetine (Prozac). Proc Natl Acad Sci USA. 2002;99:3182–7.
63. Zachariou V, Sgambato-Faure V, Sasaki T, Svenningsson P, Berton O, Fienberg AA, et al. Phosphorylation of DARPP-32 at Threonine-34 is required for cocaine action. Neuropsychopharmacology. 2006;31:555–62.
64. Svenningsson P, Fienberg AA, Allen PB, Moine CL, Lindskog M, Fisone G, et al. Dopamine D(1) receptor-induced gene transcription is modulated by DARPP-32. J Neurochem. 2000;75:248–57.
65. Håkansson K, Galdi S, Hendrick J, Snyder G, Greengard P, Fisone G. Regulation of phosphorylation of the GluR1 AMPA receptor by dopamine D2 receptors. J Neurochem. 2006;96:482–8.
66. Friedman A, Homma D, Bloem B, Gibb LG, Amemori KI, Hu D, et al. Chronic stress alters striosome-circuit dynamics, leading to aberrant decision-making. Cell. 2017;171:1191–205.e28.
67. Vialou V, Bagot RC, Cahill ME, Ferguson D, Robison AJ, Dietz DM, et al. Prefrontal cortical circuit for depression- and anxiety-related behaviors mediated by cholecystokinin: role of ΔFosB. J Neurosci. 2014;34:3878–87.
68. Langer SZ. 25 years since the discovery of presynaptic receptors: present knowledge and future perspectives. Trends Pharmacol Sci. 1997;18:95–99.
69. D'Aquila PS, Galistu A. Possible role of dopamine D1-like and D2-like receptors in behavioural activation and evaluation of response efficacy in the forced swimming test. Neuropharmacology. 2012;62:1717–29.
70. Hare BD, Shinohara R, Liu RJ, Pothula S, DiLeone RJ, Duman RS. Optogenetic stimulation of medial prefrontal cortex Drd1 neurons produces rapid and long-lasting antidepressant effects. Nat Commun. 2019;10:223.
71. Desormeaux C, Demars F, Davenas E, Jay TM, Lavergne F. Selective activation of D1 dopamine receptors exerts antidepressant-like activity in rats. J Psychopharmacol. 2020;34:1443–8.
72. Peña CJ. D1 and D2 type medium spiny neuron contributions to depression. Biol Psychiatry. 2017;81:636–8.
73. Undieh AS. Pharmacology of signaling induced by dopamine D(1)-like receptor activation. Pharmacol Ther. 2010;128:37–60.
74. Tritsch NX, Sabatini BL. Dopaminergic modulation of synaptic transmission in cortex and striatum. Neuron. 2012;76:33–50.
75. Goto Y, Grace AA. Limbic and cortical information processing in the nucleus accumbens. Trends Neurosci. 2008;31:552–8.
76. Sesack SR, Pickel VM. Prefrontal cortical efferents in the rat synapse on unlabeled neuronal targets of catecholamine terminals in the nucleus accumbens septi and on dopamine neurons in the ventral tegmental area. J Comp Neurol. 1992;320:145–60.
77. Montaron MF, Deniau JM, Menetrey A, Glowinski J, Thierry AM. Prefrontal cortex inputs of the nucleus accumbens-nigro-thalamic circuit. Neuroscience. 1996;71:371–82.
78. Brady AM, O'Donnell P. Dopaminergic modulation of prefrontal cortical input to nucleus accumbens neurons in vivo. J Neurosci. 2004;24:1040–9.
79. Grace AA, Floresco SB, Goto Y, Lodge DJ. Regulation of firing of dopaminergic neurons and control of goal-directed behaviors. Trends Neurosci. 2007;30:220–7.
80. Fischer AS, Holt-Gosselin B, Fleming SL, Hack LM, Ball TM, Schatzberg AF, et al. Intrinsic reward circuit connectivity profiles underlying symptom and quality of life outcomes following antidepressant medication: a report from the iSPOT-D trial. Neuropsychopharmacology. 2021;46:809–19.
81. Phillipson OT, Griffiths AC. The topographic order of inputs to nucleus accumbens in the rat. Neuroscience. 1985;16:275–96.
82. Khastkhodaei Z, Muthuraman M, Yang JW, Groppa S, Luhmann HJ. Functional and directed connectivity of the cortico-limbic network in mice in vivo. Brain Struct Funct. 2021;226:685–700.
83. Hikida T, Yao S, Macpherson T, Fukakusa A, Morita M, Kimura H, et al. Nucleus accumbens pathways control cell-specific gene expression in the medial prefrontal cortex. Sci Rep. 2020;10:1838.
84. Reimers JM, Milovanovic M, Wolf ME. Quantitative analysis of AMPA receptor subunit composition in addiction-related brain regions. Brain Res. 2011;1367:223–33.
85. Xue B, Mao LM, Jin DZ, Wang JQ. Pharmacological modulation of AMPA receptor phosphorylation by dopamine and muscarinic receptor agents in the rat medial prefrontal cortex. Eur J Pharmacol. 2018;820:45–52.
86. Bagot RC, Parise EM, Peña CJ, Zhang HX, Maze I, Chaudhury D, et al. Ventral hippocampal afferents to the nucleus accumbens regulate susceptibility to depression. Nat Commun. 2015;6:7062.
87. Cui Q, Li Q, Geng H, Chen L, Ip NY, Ke Y, et al. Dopamine receptors mediate strategy abandoning via modulation of a specific prelimbic cortex-nucleus accumbens pathway in mice. Proc Natl Acad Sci USA. 2018;115:E4890–9.
88. Chen H, Xiong XX, Jin SY, He XY, Li XW, Yang JM, et al. Dopamine D2 receptors in pyramidal neurons in the medial prefrontal cortex regulate social behavior. Pharmacol Res. 2024;199:107042.
89. Nathanson JL, Yanagawa Y, Obata K, Callaway EM. Preferential labeling of inhibitory and excitatory cortical neurons by endogenous tropism of adeno-associated virus and lentivirus vectors. Neuroscience. 2009;161:441–50.

AUTHOR CONTRIBUTIONS

Bingjin Li: conceptualization; supervision; funding acquisition; project administration; writing—original draft, review and editing. Ziqian Cheng: investigation; data curation; formal analysis; software; visualization; writing—original draft. Fangyi Zhao: investigation; software; visualization; methodology. Jingjing Piao: investigation; software. Wei Yang: validation; writing—review and editing. Ranji Cui: validation; writing—review and editing.

FUNDING

This work was funded by the National Natural Science Foundation of China (No. 82371540), the Jilin Province Medical and Health Talents (2019SCZT013) and Project of Jilin University Education and Teaching Reform & Research (2022JGY021).

COMPETING INTERESTS

The authors declare no competing interests.

ADDITIONAL INFORMATION

Supplementary information The online version contains supplementary material available at https://doi.org/10.1038/s41380-024-02684-5.

Correspondence and requests for materials should be addressed to Ranji Cui or Bingjin Li.